

# 1 Identification of the Mode of Evolution in 2 Incomplete Carbonate Successions

3 Niklas Hohmann<sup>\*,1,2</sup> ORCID: [0000-0003-1559-1838](https://orcid.org/0000-0003-1559-1838)

4 Joël R. Koelewijn<sup>1</sup> ORCID: [0000-0002-4668-3797](https://orcid.org/0000-0002-4668-3797)

5 Peter Burgess<sup>3</sup> ORCID: [0000-0002-3812-4231](https://orcid.org/0000-0002-3812-4231)

6 Emilia Jarochovska<sup>1</sup> ORCID: [0000-0001-8937-9405](https://orcid.org/0000-0001-8937-9405)

7

8 \*Corresponding author, email: [N.H.Hohmann@uu.nl](mailto:N.H.Hohmann@uu.nl)

9 <sup>1</sup>Utrecht University, Faculty of Geosciences, Department of Earth Sciences, Vening Meinesz  
10 building A, Princetonlaan 8A, 3584 CB Utrecht, The Netherlands.

11 <sup>2</sup>University of Warsaw, Faculty of Biology, Biological and Chemical Research Centre,  
12 Institute of Evolutionary Biology, ul. Żwirki i Wigury 101, 02-089 Warsaw, Poland.

13 <sup>3</sup>University of Liverpool, Department of Geology, Chatham St, Liverpool L69 7ZT, United  
14 Kingdom.

15

## 16 **Abstract**

17 **Background:** The fossil record provides the unique opportunity to observe evolution over  
18 millions of years, but is known to be incomplete. While incompleteness varies spatially and is  
19 hard to estimate for empirical sections, computer simulations of geological processes can be  
20 used to examine the effects of the incompleteness *in silico*.

21 We combine simulations of different modes of evolution (stasis, (un)biased random walks)  
22 with deposition of carbonate platforms strata to examine how well the mode of evolution can  
23 be recovered from fossil time series, and how test results vary between different positions in  
24 the carbonate platform and multiple stratigraphic architectures generated by different sea  
25 level curves.

### 26 **Results:**

27 Stratigraphic architecture and position along an onshore-offshore gradient has only a small  
28 influence on the mode of evolution recovered by statistical tests. Tests fail to identify the  
29 correct mode of evolution in the absence of stratigraphic effects, and support for the correct  
30 mode decreases with time series length.

31 Visual examination of trait evolution in lineages shows that rather than stratigraphic  
32 incompleteness, maximum hiatus duration determines how much fossil time series differ  
33 from the original evolutionary process. Directional evolution is more susceptible to  
34 stratigraphic effects, turning it into apparent punctuated equilibrium. In contrast, stasis  
35 remains unaffected.

### 36 **Conclusions:**

- 37 • Tests for the mode of evolution should be reviewed critically, as they do not find good  
38 support for the correct (simulated) mode of evolution, even for adequate models that

39 generated the data, in the absence of stratigraphic effects, and for exceptionally long  
40 time series.

41 • Fossil time series favor the recognition of both stasis and complex, punctuated modes  
42 of evolution.

43 • Not stratigraphic incompleteness, but the presence of rare, prolonged gaps has the  
44 largest effect on trait evolution. This suggests that incomplete sections with regular  
45 hiatus frequency and durations can potentially preserve evolutionary history without  
46 major biases. Understanding external controls on stratigraphic architectures such as  
47 sea level fluctuations is crucial for distinguishing between stratigraphic effects and  
48 genuine evolutionary process.

49

50 **Keywords:**

51 Paleontology, Stratigraphy, Trait Evolution, Paleobiology, Carbonate Platform, Mode of  
52 Evolution, Time Series, Fossil Record.

53

## 54 **Introduction**

### 55 **The fossil record as source of information**

56 Fossils provide a unique record of evolution on temporal and spatial scales not accessible to  
57 experimentation or direct human observation (Gingerich 1983; 2001). Geological records  
58 have delivered fossil time series crucial in formulating and testing hypotheses on  
59 evolutionary dynamics and mechanisms of speciation spanning micro- to macroevolutionary  
60 scales (e.g., Dzik 2005; Strömberg 2006; Aze et al. 2011; Voje 2020). Nevertheless, fossils

61 remain underused in evolutionary biology. Their main application is still calibration of  
62 molecular clocks, which commonly relies on single occurrences and is subject to biases  
63 resulting from this small sample size (Springer 1995). The unique type of information  
64 contained in a fossil succession sampled over a long time interval is rarely exploited, likely  
65 due to the following barriers:

- 66 1. The fossil record, being a part of the stratigraphic record, is patchy and distorted. At  
67 the time when Darwin (1859) discussed this as a major limitation for the testing and  
68 development of the theory of evolution, little geological knowledge was present to  
69 elucidate the rules governing this incompleteness. Darwin's concern widely persists  
70 (e.g., Patterson (1981)), albeit mostly implicitly: most phylogenetic analyses  
71 published today do not use fossils which would have been relevant or use only a small  
72 fraction of them. Stratigraphy and sedimentology, which can provide relevant data on  
73 fossils and the constraints on their occurrence and sampling (Kidwell and Holland  
74 2002; Hunt 2010), are jargon-laden, highly atomized disciplines whose utility for  
75 evolutionary biology is not obvious to biologists. Biostratigraphy, which uses fossil to  
76 establish the relative age of rocks and has amassed datasets that would be of high  
77 utility for evolutionary studies, employs taxonomic concepts that are often impractical  
78 for or incompatible with evolutionary questions (Dzik 1985; 1995; Pearson 1992;  
79 Haug and Haug 2017). As a results, scientific communities studying evolution and the  
80 fossil record function in parallel, with limited exchange (Grantham 2004).
- 81 2. There is a lack of methodological frameworks to incorporate fossils in evolutionary  
82 studies. Historically, phylogenetic methods rarely incorporated geological information  
83 such as the relative order of appearance of taxa or specimens in the fossil record,  
84 which is the main subject of biostratigraphy (Wills 1999). This has led to radical  
85 discrepancies between the outcomes of phylogenetic and stratigraphic, or

86 stratophenetic, approaches (Gingerich and Schoeninger 1977; Donoghue 2001; Dzik  
87 2005). This barrier is gradually overcome by methodological advances, such as the  
88 Fossilized Birth-Death Model (Stadler et al. 2018), which allows incorporation of  
89 parameters specific to the fossil record, such as fossilization rate, sampling probability  
90 and age uncertainties of fossil occurrences (Barido-Sottani et al. 2020; Warnock,  
91 Heath, and Stadler 2020; Wright et al. 2022; Barido-Sottani et al. 2023).

92 Recently, there is renewed appreciation for the importance of fossils in phylogenetic  
93 reconstructions (Quental and Marshall 2010; Mitchell, Etienne, and Rabosky 2019;  
94 Mongiardino Koch, Garwood, and Parry 2021; Guenser et al. 2021). These studies focus on  
95 the role of the morphological information provided by extinct taxa, but less on what a modern  
96 understanding of the physical structure of the geological record contributes to reconstructing  
97 evolutionary processes from fossil-bearing stratigraphic successions.

## 98 **Stratigraphic incompleteness and age-depth models**

99 The incompleteness of the fossil record serves as an umbrella term for different effects that  
100 diminish the information content of the rock record, ranging from taphonomic effects and  
101 sampling biases to the role of gaps and erosion (Kidwell and Holland 2002). Here we focus  
102 on the role of gaps (hiatuses) in the rock record. Such gaps can arise due to sedimentation  
103 (including fossils) and subsequent erosion or lack of creation of rocks in the first place, e.g.  
104 when an environment remains barren of sediment formation or supply for a long time. Both  
105 processes result in gaps in the rock record and, as a result, in the fossil record. This type of  
106 incompleteness is termed stratigraphic (in)completeness, defined as the time (not) recorded in  
107 a section, divided by the total duration of the section (Dingus and Sadler 1982; Tipper 1987).  
108 Stratigraphic completeness provides an upper limit on the proportion of evolutionary history  
109 that can be recovered from a specified section, even with unlimited resources and perfect

110 preservation of fossils. Stratigraphic completeness is difficult to quantify in geological  
111 sections, and estimates range between 3 and 30 % (Wilkinson, Opdyke, and Algeo 1991),  
112 suggesting that more than 70 % of evolutionary history is either not recorded in the first place  
113 or destroyed at a later time.

114 Fossils older than a 1.5 million years cannot be dated directly, and their age has to be inferred  
115 from circumstantial evidence on the age of the strata in which they were found (Wehmiller et  
116 al. 1988; Kidwell and Flessa 1996). This inference is formalized by age-depth models  
117 (ADMs), which serve as coordinate transformations between the stratigraphic domain, where  
118 the fossils were found (length dimension L, SI unit meter), and the time domain (time  
119 dimension T, SI unit seconds - we use the derived units years, kyrs, or Myrs) (Hohmann  
120 2021). Age-depth models are always explicitly or implicitly used when fossil data is used for  
121 evolutionary inferences. Because they convey how positions of fossils relate to their age,  
122 ADMs are the basis for calculating evolutionary rates. As a result, revising ADMs commonly  
123 leads to a revision of evolutionary rates. For example, Malmgren, Berggren, and Lohmann  
124 (1983) observed increased rates of morphological evolution in lineages of fossil foraminifera  
125 over a geologically short time interval of 0.6 Myr and proposed that this “punctuated  
126 gradualism” may be a “common norm for evolution”. MacLeod (1991) revised the age-depth  
127 model and showed that the interval with increased rates of evolution coincides with a  
128 stratigraphically condensed interval, i.e. more change is recorded in a thinner rock unit. Re-  
129 evaluating the evolutionary history based on the revised age-depth model removed the  
130 apparent punctuation and showed that morphological evolution in that case had been gradual  
131 rather than punctuated.

132 Age-depth models contain information on both variations in sediment accumulation rate and  
133 gaps in the stratigraphic and - as a result – the fossil record. For example, stratigraphic  
134 completeness corresponds to the fraction of the time domain to which an age-depth model

135 assigns a stratigraphic position. In the absence of an age-depth model, we can only make  
136 statements on the ordering of evolutionary events, but not on the temporal rates involved.

## 137 **Forward models of stratigraphic architectures**

138 Forward computer simulations of sedimentary strata provide a useful tool to study the effects  
139 of incompleteness and heterogeneous stratigraphic architectures. They have demonstrated  
140 that locations and frequency of gaps in the stratigraphic record are not random, but a  
141 predictable result of external controls, such as fluctuations in eustatic sea level (Warrlich  
142 2000; Hutton and Syvitski 2008; Burgess 2013; Masiero et al. 2020).

143 Combined with biological models, forward models provide a powerful tool to test hypotheses  
144 on the effects of stratigraphic architectures on our interpretations of evolutionary history. For  
145 example, Hannisdal (2006) combined simulations of a siliciclastic basin with models of  
146 taphonomy and phenotypic evolution. The results showed that when sample sizes are small,  
147 morphological evolution will appear as stasis regardless of the underlying mode. This might  
148 explain why stasis is the most common evolutionary pattern recovered from the fossil record  
149 (Hunt, Hopkins, and Lidgard 2015).

150 Stratigraphic incompleteness and variations in sediment accumulation rates introduce  
151 multiple methodological challenges. Constructing complex ADMs requires sedimentological  
152 and stratigraphic expert knowledge, and they will potentially be associated with large  
153 uncertainties. Even in the “perfect knowledge” scenario where the age-depth model is fully  
154 known, evolutionary history in the time domain will inevitably be sampled irregularly: If two  
155 samples are separated by a hiatus, their age difference must be at least the duration of the  
156 hiatus, which might be millions of years. On the other hand, if sediment accumulation is rapid  
157 and no hiatuses are present, the age difference between samples might be only a few days.

158 Most studies “translate” fossil successions into time series using age-depth models based on  
159 simplified assumptions on the regularity of the stratigraphic record. These ADMs ignore  
160 stratigraphic incompleteness and often assume uninterrupted constant sediment accumulation  
161 (UCSA). This assumption implies that stratigraphic completeness is 100 %, rock thickness is  
162 proportional to time passed, and linear interpolation between tie points of known age can be  
163 used to infer fossil ages from their positions. Such ADMs are usually used implicitly, without  
164 discussing their limitations. While the assumption of UCSA is sedimentologically and  
165 stratigraphically unrealistic, it brings strong methodological simplifications. For example, if  
166 distance between samples collected in a rock section is kept constant, UCSA implies that the  
167 underlying evolutionary history in the time domain is sampled at a constant frequency, the  
168 generated fossil time series are equidistant in time and can therefore be analyzed by standard  
169 methods of time series analysis (Hunt 2006; Beran 2017).

## 170 **Objectives and hypotheses**

171 We examine how commonly made simplified assumptions on stratigraphic architectures  
172 influence how the mode of evolution is recovered from fossil time series. We use tropical  
173 carbonate platforms as a case study, because they host large parts of the fossil record and are  
174 evolutionary hotspots (Jablonski, Roy, and Valentine 2006).

175 We test the following hypotheses:

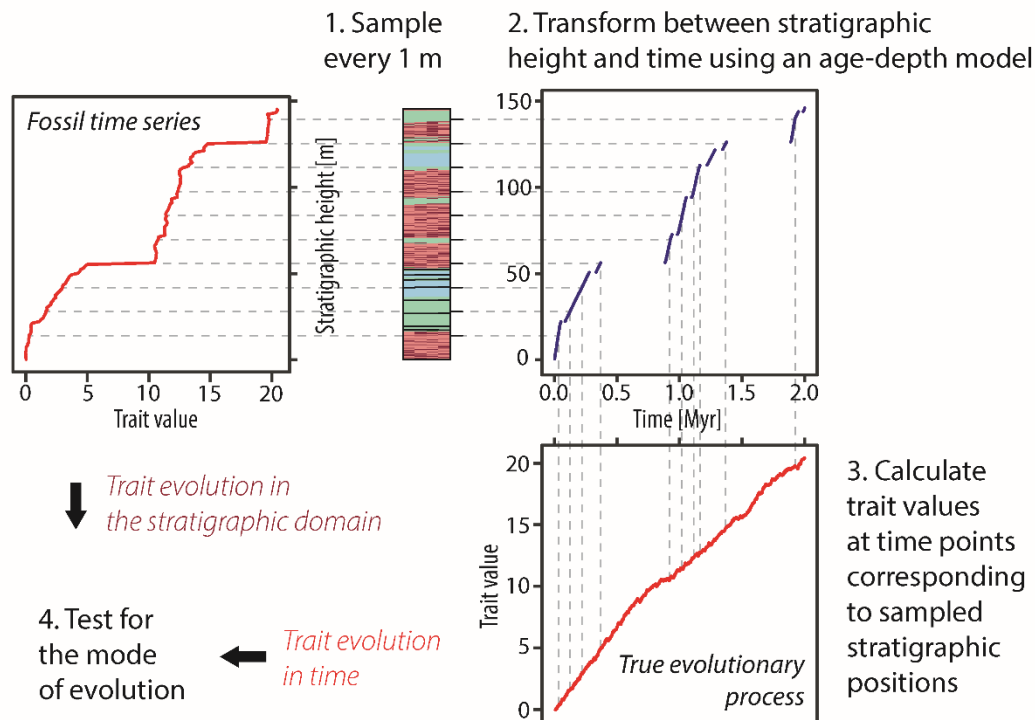
- 176 1. The mode of evolution identified in a fossil time series obtained under the assumption  
177 of uninterrupted constant sediment accumulation (UCSA) is the same as the mode of  
178 the original time series.
- 179 2. Lower stratigraphic completeness reduces the chance of identifying the correct mode  
180 of evolution from fossil time series constructed based on the assumption of UCSA.



181           The implication of this hypothesis is that different depositional environments have  
182           different chances of preserving the mode of evolution because of systematic  
183           differences in their completeness.

## 184   **Methods**

185   We simulate trait evolution in the time domain, pass it through a stratigraphic filter produced  
186   by the CarboCAT Lite model of carbonate platform formation (Burgess 2013; Burgess 2023),  
187   and compare how well the mode of evolution can be recovered from the fossil time series  
188   sampled in the stratigraphic domain and the time series reflecting the “true” evolutionary  
189   history in the time domain. A visual summary of the workflow is shown in [Figure 1](#). Data is  
190   available in Hohmann, Koelewijn, and Jarochowska (2023a), code is available Hohmann,  
191   Koelewijn, and Jarochowska (2023b). See the README and REPRODUCEME files therein  
192   for details on computational reproducibility.



193

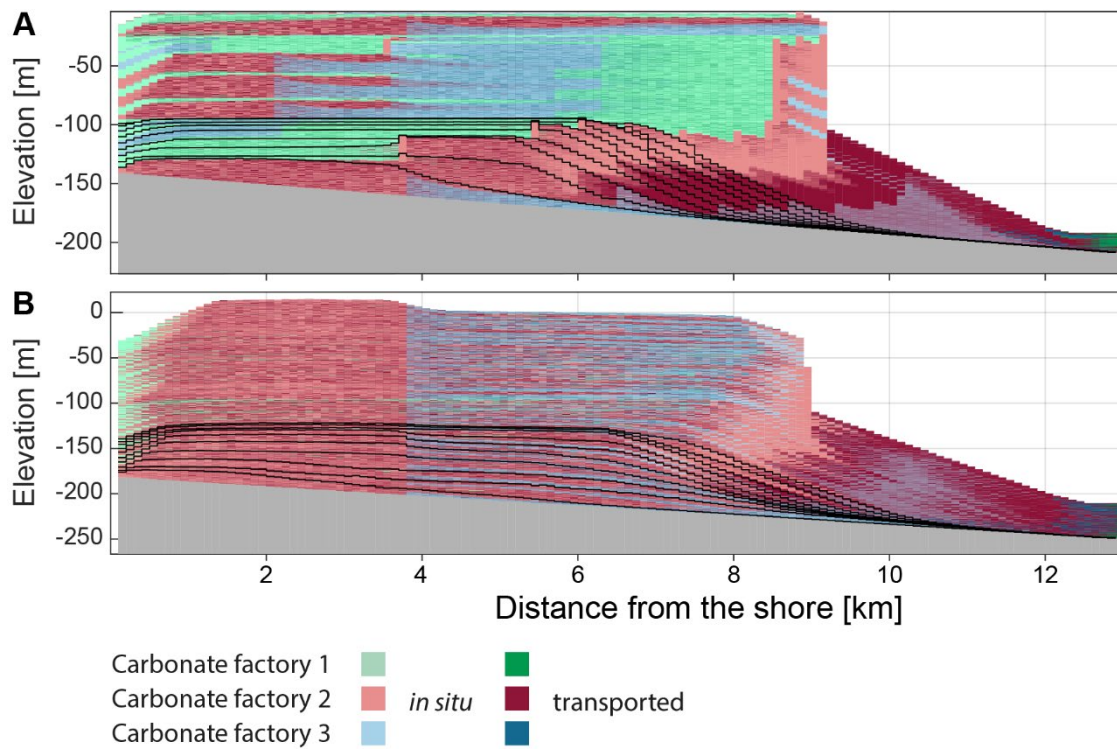
194 *Figure 1: Study design for testing the mode of evolution in the stratigraphic domain.*

195 *Computationally, first sampling positions are determined, then the age-depth model is used to*  
196 *determine the times that correspond to these positions. Last, the trait evolution at said times*  
197 *are simulated. The simulated mean trait values are the values observable at the sampled*  
198 *stratigraphic positions.*

## 199 **The stratigraphic record: Forward models of carbonate** 200 **platform architecture**

201 We simulated two attached carbonate platforms using the CarboCAT Lite software ([Figure 2](#)  
202 and [Figure 3](#)) (Burgess 2023). CarboCAT Lite is implemented in MATLAB and simulates  
203 carbonate production by carbonate factories characterized by different production curves,  
204 which are functions of water depth (Bosscher and Schlager 1992; Burgess 2013; Masiero et  
205 al. 2020). It includes sediment transport that is a function of platform topography, i.e.,

206 sediment is transported downslope, but not a function of external parameters such as waves  
207 or currents. Simulations were run using time steps of 1 kyr (1000 years) and a grid of 1 km  
208 width (strike) and 15 km length (dip), subdivided into quadratic grid cells of 100 m length.  
209 We used three carbonate factories with production curves following the parametrization of  
210 Bosscher and Schlager (1992) (*Supplementary Figure 1*). Factory 1 is phototrophic with a  
211 maximum carbonate production rate of  $500 \text{ m} \times \text{Myr}^{-1}$ , which it maintains up to 30 m of  
212 water depth. Factories 2 and 3 have maximum production rates of 160 and  $150 \text{ m} \times \text{Myr}^{-1}$   
213 respectively and maintain maximum productivity until 40 m water depth, but differ in how  
214 fast productivity decreases with depth (*Supplementary Figure 1*). We assumed constant  
215 subsidence of 70 m per Myr across the grid. This is approximately seven times higher than  
216 estimated subsidence rates in the last 125 kyr in the Bahamas (McNeill 2005), allowing for  
217 higher completeness than would be generated on a typical passive continental margin. As  
218 initial topography, a slope with a gradient of  $5.33 \text{ m} \times \text{km}^{-1}$  was used, resulting in a total  
219 initial difference in water depth of 80 m between the shore and the offshore end of the  
220 simulated grid. We followed the default setting of CarboCAT Lite, described by Burgess  
221 (2013) with three lithofacies (sediment types) corresponding to the three carbonate factories,  
222 plus three secondary lithofacies representing sediment transported downslope after the  
223 deposition of the primary lithofacies (dark colors in *Figures 2* and *3*). As initial facies  
224 distribution, the default setting of CarboCAT Lite was used, which assigns each grid cell one  
225 of the three carbonate factories or no factory according to a uniform distribution.



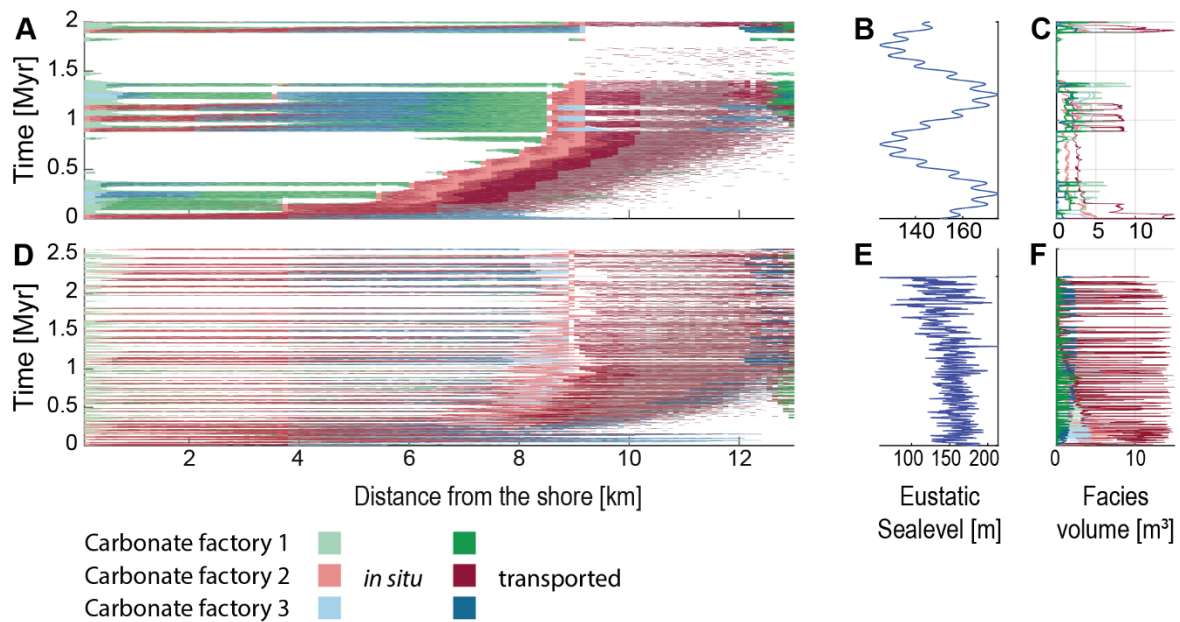
226

227 *Figure 2: The outcome of simulating carbonate platforms in the stratigraphic domain. (A)*

228 *Scenario A: deposition based on a fictional sea-level curve. (B) Scenario B: deposition based*

229 *on the sea-level curve from Miller et al. (2020) for the last 2.58 Myr. Graphs represent the*

230 *position in the middle of the simulated grid along the strike.*



231

232 *Figure 3: Simulated carbonate platforms in the time domain. (A-C) Scenario A. (D-F)*  
233 *Scenario B. (A, D) Chronostratigraphic (Wheeler) diagrams. (B, E) Sea level curves used as*  
234 *input for the simulation. (C, F) Facies volumes. Graphs represent the position in the middle*  
235 *of the simulated grid along the strike.*

236 Two scenarios were simulated (Figures 2 and 3). In scenario A, the simulation was run for 2  
237 Myr with changes in eustatic sea level given by a combination of sinusoids expressed as  
238 third-order sea level changes with a period of 1 Myr and an amplitude of 20 m and fourth-  
239 order changes with a period of 0.112 Myr and an amplitude of 2 m (Figure 3 B). Scenario B  
240 was simulated for the period from 2.58 Mya (beginning of the Pleistocene) until the present  
241 using the global eustatic sea level curve estimated from global  $\delta^{18}\text{O}_{\text{benthic}}$  records by Miller et  
242 al. (2020). This curve has a temporal resolution of approximately 2 kyr over the Pleistocene  
243 (mean: 2.13 kyr, median: 2.07 kyr), and was linearly interpolated to match the time  
244 increments of the simulation and normalized to have a mean sea level of 0 (Figure 3 E).  
245 For each scenario, CarboCAT Lite produces a grid containing the facies, including no  
246 deposition, at each time step and position on the grid. The outputs were extracted from

247 MATLAB and all further analysis was carried out in the R Software (R Core Team 2023).  
248 For both scenarios, age-depth models at every grid node were extracted from the simulation  
249 outputs. Age-depth models taken from the same distance from shore display only little  
250 variation as position along the shore (strike) is varied, indicating that lateral position in the  
251 grid is negligible. Accordingly, we focused on age-depth models taken from the middle  
252 transect along the dip. In each scenario, synthetic sections and the corresponding age-depth  
253 models at five locations were selected (*Supplementary Figure 2*). The selected locations are 2  
254 km, 6 km, 8 km, 10 km, and 12 km from the shoreline. These distances corresponded to  
255 lagoonal environments, backreef, forereef, proximal slope, and distal slope. The simulated  
256 carbonate platforms accreted vertically with only minor shift of environments along the  
257 onshore-offshore axis, therefore each location can be interpreted as representing its respective  
258 environment across the entire simulation (platform lifetime). Only simulation outputs  
259 between the shore and 13 km offshore are shown in the figures, as the remainder (13-15 km)  
260 consisted entirely of redeposited carbonates and was not used further.

261 The simulated carbonate platforms were characterized using the following parameters  
262 calculated at any given location in the platform:

- 263 1. Stratigraphic completeness, calculated as the proportion of time steps with sediment  
264 accumulation relative to the total number of time steps in the simulation (function  
265 `get_completeness` in Hohmann, Koelewijn, and Jarochowska (2023b)),  
266 corresponding to completeness on the time scale of 1 kyr (Tipper 1987; Anders,  
267 Krueger, and Sadler 1987; Kemp 2012)
- 268 2. Distribution of hiatus durations in Myr (function `get_hiatus_distribution` in  
269 Hohmann, Koelewijn, and Jarochowska (2023b))

## 270 **Simulation of phenotypic trait evolution in the time**

### 271 **domain**

272 We simulated three commonly discussed modes of evolution in the time domain: stasis,  
273 unbiased random walk, and biased random walk (Hunt 2006; Jones 2009; Hopkins and  
274 Lidgard 2012; Hunt, Hopkins, and Lidgard 2015). These simulations serve as “true”  
275 evolutionary history against which we compare fossil time series derived under simplified  
276 assumptions on age-depth models.

277 In unbiased random walk models, the change in traits over a fixed time step is independent of  
278 the previous trait values, and drawn from a distribution with mean zero (Bookstein 1987;  
279 Sheets and Mitchell 2001). In biased random walk models, the mean can deviate from zero.  
280 The trait evolution along a lineage is then generated by summing up the incremental changes  
281 in traits. Commonly used models of random walks are based on equidistant time steps,  
282 meaning the time passed between two observations of the random walk is identical for all  
283 observations. We could not use these models, because depending on where in the  
284 stratigraphic column samples are collected, the time elapsed between two successive  
285 sampling positions can vary by more than three orders of magnitude. It will be less than a  
286 thousand years when sediment accumulation rate is high, and more than half a million years  
287 when they are separated by a hiatus ([Figure 4](#)). If samples have identical distances in the  
288 stratigraphic column, the underlying evolutionary history will be sampled at irregular times.  
289 We use continuous-time extensions of random walk and stasis models so we can sample  
290 lineages at arbitrary time points without relying on interpolation between discrete time steps.  
291 Interpolation would potentially introduce dependencies between successive samples,  
292 contradicting the assumption of the random walk model that change in traits is independent

293 and identically distributed. The continuous-time expansion provides exact trait values at the  
294 sampled times, and reduces to the standard discrete time step models when applied to  
295 equidistant time steps. In addition, discrete-time models incorporate time elapsed between  
296 observations into model parameters (e.g., the variance parameter of the random walk model),  
297 making their scaling behavior non-obvious when time scales are varied. Using continuous-  
298 time implementations makes it possible to compare observations across time scales and vary  
299 the granularity of observation while keeping the underlying model of evolution identical. We  
300 use this property to examine how increased sampling of the same time interval influences  
301 model selection performance. Another commonly considered mode is the Ornstein-  
302 Uhlenbeck (OU) process, which corresponds to noisy convergence towards a trait optimum  
303 (Lande 1976). The stochastic differential equations describing Ornstein-Uhlenbeck are  
304 usually solved using the Euler-Maruyama method with equidistant time steps (Platen and  
305 Bruti-Liberati 2010). We did not simulations of OU processes due to the difficulty of  
306 generating heterodistant samples (samples not equally spaced in time) from them.

307 We extracted age-depth models from CarboCAT Lite outputs. The age-depth models serve as  
308 functions  $H : L \rightarrow T$  that connect the stratigraphic domain  $L$  with the time domain  $T$ . Given a  
309 model of trait evolution  $M_t$  in the time domain, we then define its stratigraphic expression as  
310  $M \circ H^l$ , which is the trait evolution observable in the stratigraphic column. This allows us to  
311 form triplets  $(h, t, m)$ , where  $h$  is a stratigraphic position,  $t$  is the time when that position was  
312 formed, and  $m$  is the trait value that describes the true evolutionary history at time  $t$  and can  
313 be observed at height  $h$  (*Figure 1*). The R package DAIME (Hohmann 2021) was used for  
314 age-depth transformations to sample time and depth domain at arbitrary points. The  
315 theoretical underpinning for the need of these transformations can be found in Hohmann  
316 (2021). For the (un)biased random walk models, we use Brownian drift as a continuous-time  
317 expansion. It is given by



318 
$$X_t = \mu \cdot t + \sigma B_t$$

319 where  $\mu$  and  $\sigma$  are model parameters,  $t$  is time, and  $B_t$  is a Brownian motion. The parameter  $\mu$   
320 specifies how biased or directional the Brownian drift is and  $\sigma$  specifies how volatile the  
321 process is. After  $t$  time units have passed, the distribution of a trait following a Brownian drift  
322 model is normally distributed with standard deviation  $\sigma$  and mean  $\mu \times t + x_0$ , where  $x_0$  is the  
323 trait value at the beginning of the observation. When sampled at equidistant points in time,  
324 this reduces to a standard random walk model where a normal distribution determines the  
325 step sizes.

326 Stasis is expressed as the lack of net change in traits over the period of observation. We  
327 model stasis as a series of independent, identically distributed random variables with mean  $m$   
328 and standard deviation  $s$  (Sheets and Mitchell 2001). As a result, stasis is not affected by the  
329 heterodistant sampling in the time domain.

330 We examined the preservation of four evolutionary scenarios (*Supplementary Figure 3*):

- 331 (1) Stasis with mean  $m = 0$  and standard deviation  $s = 1$ ;  
332 (2) Brownian motion as a special case of Brownian drift with parameters  $\mu = 0$  and  $\sigma = 1$ ;  
333 (3) weak Brownian drift with parameters  $\mu = 5$  and  $\sigma = 1$ , corresponding to a weakly  
334 directional random walk;  
335 (4) strong Brownian drift with parameters  $\mu = 10$  and  $\sigma = 1$ , corresponding to a strongly  
336 directional random walk.

337 After one million years of evolution, the Brownian motion has an expected change in traits  
338 of zero, while the weak and strong Brownian drift have an expected change of traits of 5 and  
339 10, respectively. For comparability, the  $\sigma$  parameter on the Brownian motion and drift  
340 models was kept constant, resulting in a standard deviation of traits around their mean value

341 equal to one after one million years. The four evolutionary scenarios differ in their  
342 directionality, defined as the difference in traits accumulated over time. While weak and  
343 strong Brownian drift are directional, stasis and Brownian motion on average are not.  
344 Individual lineages following a Brownian motion can deviate drastically from their initial  
345 trait value – only when multiple lineages are observed, the mean trait values observed in  
346 them average to zero (*Supplementary Figure 3*).

## 347 **Sampling procedure in the stratigraphic domain**

348 For clarity, we distinguish between fossil time series and time series. Fossil time series are  
349 taken in the stratigraphic domain and record trait values observed at specific stratigraphic  
350 positions, whereas time series are located in the time domain and record trait values observed  
351 at specific points in time.

352 To isolate the effects of stratigraphic incompleteness, we assume all lineages have an equal  
353 chance of being sampled across all environments. We assume identical sampling procedures  
354 for fossil time series in both scenarios: a sample is taken every meter and consists of 100  
355 specimens. The distribution of traits among the specimens in a sample is normally distributed  
356 with variance of 0.1 and a mean according to the simulated trait values. This choice is made  
357 so the fossil time series match the format required by the paleoTS package (Hunt 2006;  
358 2022), which we use to identify the mode of evolution. The variance of 0.1 was chosen to  
359 ensure that variability within a sample is small compared to the expected mean evolutionary  
360 change that accumulates over the course of the simulations, thus reducing the chance to  
361 mistake variability within populations for evolutionary trends (Hannisdal 2006). This  
362 procedure generates equidistant fossil time series with, depending on the location in the  
363 platform, 20 to 150 sampling positions in scenario A and 50 to 220 sampling positions in

364 scenario B. This is more than most studies with stratophenetic datasets (Clyde and Gingerich  
365 1994; Dzik 1999; Hunt and Roy 2006). For example, fossil time series compiled by Hunt,  
366 Hopkins, and Lidgard (2015) had a median of 14 sampling positions and the longest fossil  
367 time series consisted of 114 sampling positions.

## 368 Identification of the mode of evolution from simulated fossil time 369 series

370 We applied the tests for the mode of evolution implemented in the `compareModels`  
371 function of the `paleoTS` package version 0.5.3 (Hunt 2022) to the simulated stratigraphic  
372 series. The tests use corrected Akaike's Information Criterion (AICc) to determine which of  
373 the following models fits best to the fossil time series: the stasis model, an unbiased random  
374 walk (URW), a biased random walk referred to as general random walk (GRW), and an  
375 Ornstein-Uhlenbeck process (OU). While we did not simulate Ornstein-Uhlenbeck processes,  
376 we included it in the set of tested models as it corresponds to a distinct mode of evolution  
377 (convergence to a phenotypic optimum). The models identified by the `compareModels`  
378 function correspond to the simulated processes as follows: URW to the Brownian motion,  
379 GRW to the weak and strong Brownian drift, and stasis to stasis. The tests take the between-  
380 samples variance in trait values and the number of specimens found at a sampling position  
381 into account. At each location in the carbonate platform, 100 fossil time series per  
382 evolutionary scenario (stasis, Brownian motion, weak and strong Brownian drift) were  
383 simulated and tested for their fit to the stasis, URG, GRW, and OU model. Because raw AICc  
384 values carry no meaning, we use the derived AICc weights instead. The (uncorrected) AIC  
385 weight of a model can be interpreted as the probability that it is the best approximating  
386 model, given the data and the set of candidate models (Wagenmakers and Farrell 2004). Thus  
387 higher AIC weights (and, as a result, AICc weights) reflect better support for the model. We

388 considered a model as identified by the paleoTS package if it is in the 90 % confidence set of  
389 models (Symonds and Moussalli 2011), meaning its AICc weight is higher than 0.9, making  
390 it a single best model according to Portet (2020).

391 As a baseline for the test performance of the paleoTS package, the tests were also performed  
392 in the time domain, i.e. without any losses or distortions introduced by the stratigraphic  
393 record. To this aim, the time interval of observation (2 Myr and 2.56 Myr for scenario A and  
394 B, respectively) was subdivided into 5, 10, 15, 20, 25, 35, 50, 100 and 200 equally spaced  
395 sampling points. Lineages evolving according to the specified modes of evolution were  
396 sampled at these time points, and the test for the modes of evolution was performed on the  
397 resulting time series. Our hypothesis for this baseline is that in the absence of stratigraphic  
398 effects, increased sampling effort (i.e., a higher number of subdivisions of the time interval of  
399 observation, resulting in longer time series) increases support for the correct mode of  
400 evolution.

## 401 **Results**

### 402 **Stratigraphic architectures**

#### 403 **Carbonate platform A**

404 Platform A ([Figure 2 A](#); [Figure 3 A-C](#)) has a steep topography with high build-up up to 8 km  
405 into the basin and thin, condensed off-platform deposits between 8 and 13 km, consisting  
406 mostly of transported sediment. The majority of transported sediment is derived from the  
407 phototrophic factory, with a sharp drop in production rate at around 30 m water depth

408 (*Supplementary Figure 1*). The thinnest interval at ca. 13 km into the basin contains also  
409 sediment transported from the two other factories.

410 The platform consists of two “depositional sequences” with different topographies. These  
411 “sequences” correspond to two sea-level highs, with the first one resulting in low topography  
412 and rapid progradation that led to basinward, rather than upward, growth of the platform. The  
413 second “sequence” is aggradational, with distinct “parasequences” expressed in facies,  
414 corresponding to the 125 kyr period in the sea-level curve used as simulation input. This  
415 “sequence” is responsible for the steep topography of the platform. The top of the platform is  
416 abruptly truncated as a result of the long-term cycle sea-level fall and covered with a thin  
417 deposit of the ensuing initial transgression.

418 The two long-term cycle sea-level falls result in two major gaps ([Figure 3 A](#)). The gap  
419 between the first and the second “depositional sequence” does not extend uniformly across  
420 the entire platform. During the time of the gap formation, the euphotic factory and sediment  
421 derived from transport of this factory’s products accumulated at the platform edge,  
422 prograding between 5 and 12 km basinward. The last part of this interval offlaps the platform,  
423 forming an architecture resembling the Falling Stage Systems Tract (Plint and Nummedal  
424 2000). In contrast, the second major gap resulted in almost no deposition, reflecting almost  
425 no sediment transport in the second stage of platform formation. As a result, this platform is  
426 characterized by: two long gaps in deposition and several shorter gaps with limited spatial  
427 extent; large differences in thickness along the onshore-offshore gradient and a substantial  
428 contribution of sediment transport and offshore deposits formed entirely from sediment  
429 exported from the platform in the first half of the platform formation.

## 430 **Carbonate platform B**

431 For scenario B, we used the Pleistocene-Holocene global mean sea-level estimate of Miller et  
432 al. (2020). In the original dataset, the sea level varied between -121 m to 31.9 m and was here  
433 normalized to a mean of 0 m ([Figure 3 E](#)). The simulated time interval corresponds to  
434 gradually lowering global sea level dominated by 41-ka tilt forcing leading to amplitudes  
435 reaching 50 m. A gradual increase in sea-level amplitude throughout this interval is attributed  
436 to the onset of the glaciation of the Northern Hemisphere. In the middle Pleistocene, ca. 800  
437 ka, a shift to “quasi-100-ka” periodicity is associated with higher sea level amplitudes  
438 reaching 140 m (Miller et al. 2020). This Milankovitch-paced sea-level changes resulted in a  
439 simulated carbonate platform with short gap durations ([Figure 3 D](#), [Figure 4 B](#)). Where  
440 present, the gaps are widespread across the platform, i.e. sea-level drops resulted in gaps  
441 uniformly distributed across all environments. The continuity of gaps is even more  
442 pronounced in the youngest part of the platform corresponding to the last 800 kyr, reflecting  
443 the higher sea-level amplitude. Most gaps are concentrated in the central part of the platform,  
444 whereas the most shore- and basinward parts of the platform may be filled with sediment at  
445 the time when no other strata is formed in the grid, leading to the highest completeness of  
446 these two opposite ends. The dominant facies is sediment transported from the phototrophic  
447 factory (dark red in [Figure 2](#)), which is present across the entire platform, rather than  
448 exported off the platform as in scenario A. Hence, this platform is dominated by short-  
449 distance sediment transport. In the older part of the platform, the offshore part (at a distance  
450 of 11-13 km from the shore) has a higher stratigraphic completeness (more time represented  
451 by sediment) than the onshore end, but in the younger part of the platform, the difference  
452 disappears. The lack of large sea-level falls results in a lack of major facies shifts, low  
453 topography and a gradual, nearly aggradational buildup ([Figure 2 B](#)).

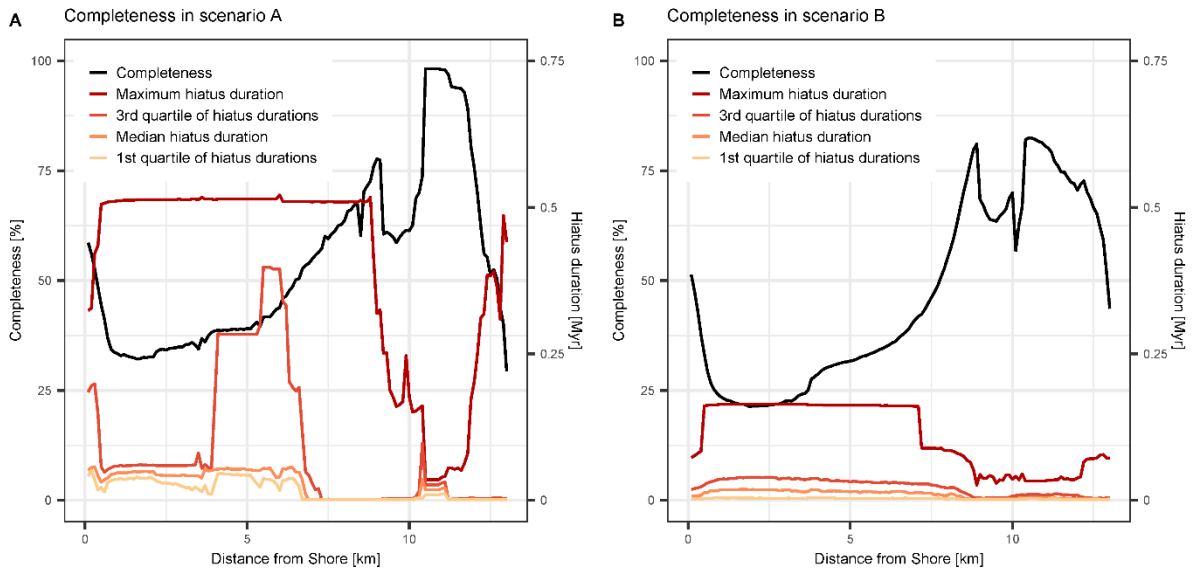
## 454 **Completeness and distribution of hiatuses**

455 Changes in completeness along the onshore-offshore gradient were very similar for both  
456 scenarios: completeness increased monotonously from the shore and had a double peak  
457 around 9 and 11 km offshore, where it reached values of 75 and 95 percent (onshore and  
458 offshore peak) in scenario A and around 80 percent (both peaks) in scenario B ([Figure 4](#)).

459 The onshore peak in completeness coincided with the forereef environment, where organisms  
460 continuously grow, while the second peak coincided with the slope onset, where transported  
461 sediment is continuously provided by the forereef. Average completeness across the platform  
462 was 53.7 % in scenario A and 46.3 % in scenario B, completeness was lowest 13 km from  
463 shore in scenario A and 1.9 km from shore in scenario B.

464 Qualitatively, the distribution of hiatus durations was similar for both scenarios. Maximum  
465 hiatus duration was constant over the entire platform, dropped dramatically on the slope, and  
466 then increased again off-platform. The first quartiles, medians and third quartiles of hiatus  
467 durations differed substantially from maximum hiatus durations. The exception to this is the  
468 backreef in scenario A (approx. 4–6 km from shore), where the 3<sup>rd</sup> quartile of hiatus durations  
469 reaches values of 0.25 to 0.4 Myrs. Averaged over the platform, maximum hiatus duration is  
470 one to two orders of magnitude larger than median hiatus duration (135 times longer in  
471 scenario A and 13 times longer in scenario B). This shows that the distribution of hiatus  
472 durations on the platform is heavy-tailed: most hiatuses are short, but a few exceptionally  
473 long hiatuses that are associated with long-term drops in sea level are present.

474 Quantitatively, hiatus durations in scenario A are longer (average median hiatus duration  
475 across the platform: 26 kyr in scenario A, 10 kyr in scenario B). The maximum hiatus  
476 duration is on average almost four times higher in scenario A than in scenario B.



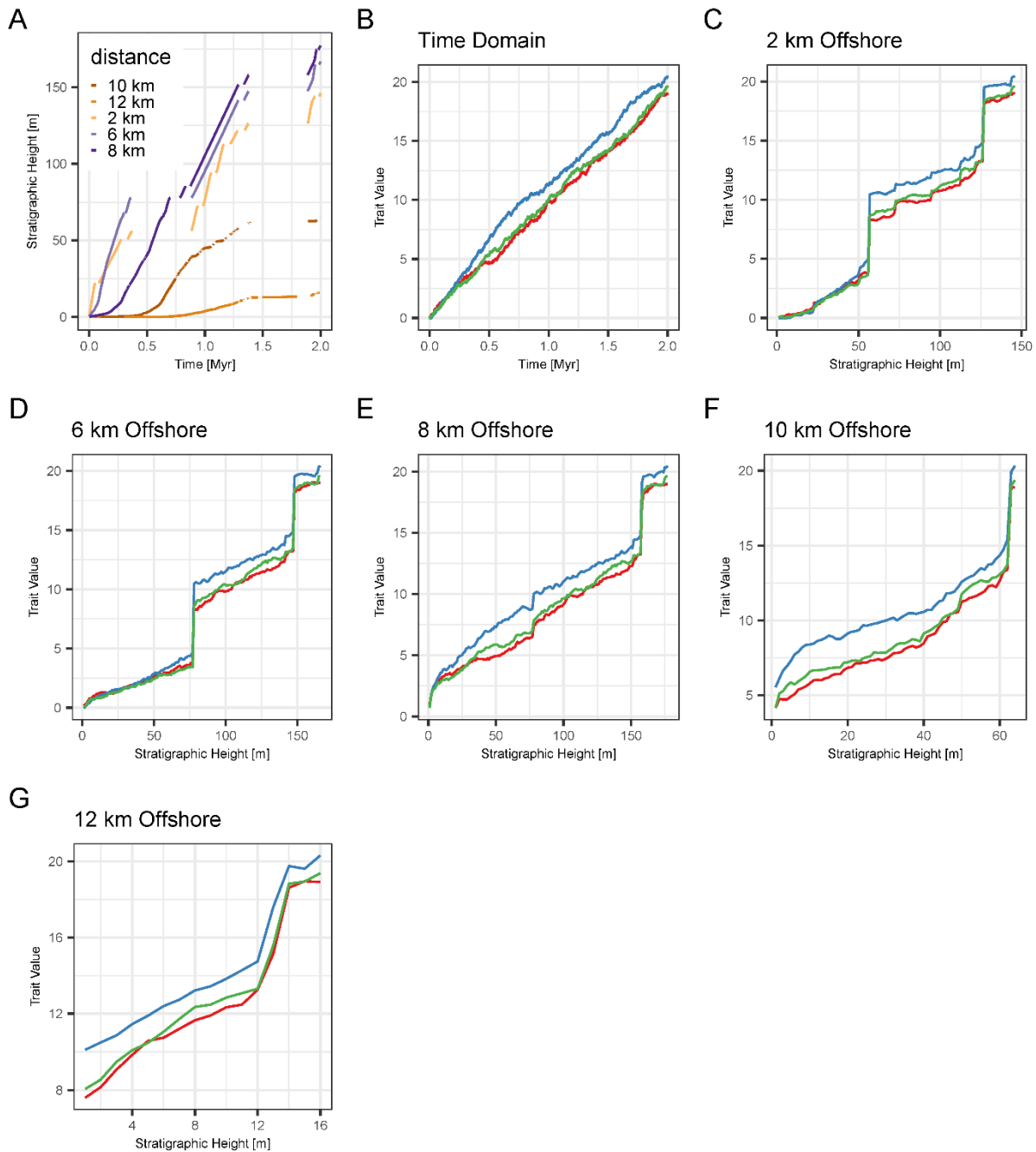
477

478 *Figure 4: Stratigraphic completeness and distribution of hiatus durations along the onshore-*  
479 *offshore gradient in scenario A (left) and B (right). Maximum hiatus duration in scenario B is*  
480 *four times lower than in scenario B, while completeness is comparable.*

## 481 **Stratigraphic expression of evolution**

482 Overall, we find that stratigraphic effects on the preservation of the mode of evolution are  
483 spatially heterogeneous within the carbonate platforms ([Figure 5](#)), and strongly depend on (1)  
484 the directionality of the examined mode of evolution ([Figure 6](#)) and (2) the presence of  
485 single, long hiatuses rather than the stratigraphic completeness at the location where the fossil  
486 time series is sampled ([Figure 7](#)). As a result, under high-frequency sea-level changes  
487 (scenario B), trait evolution is much more similar to true evolutionary change in the time  
488 domain than under slow-frequency sea-level changes (scenario A).



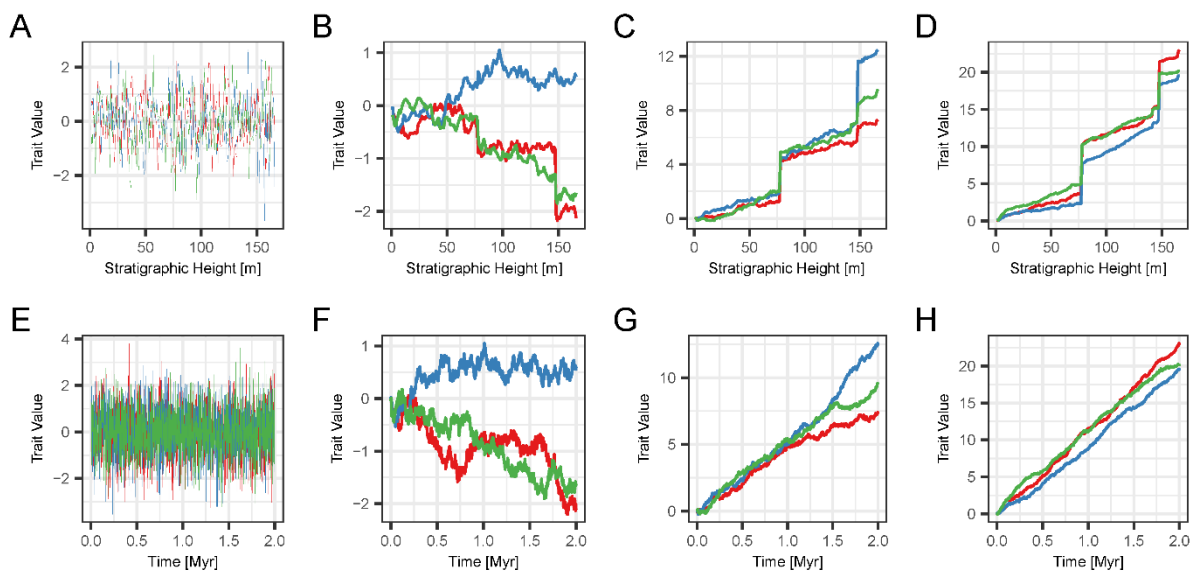


489

490 *Figure 5: Spatial variability of the preservation of evolution in scenario A. (A) Age-depth*  
491 *models at varying distances from shore (B) three simulations of strong Brownian drift in the*  
492 *time domain (C), (D), (E), (F), (G) preservation of the lineages from (B) in the stratigraphic*  
493 *domain at 2 km, 6 km, 8 km, 10 km, and 12 km from shore in platform A. The same*  
494 *evolutionary history (B) is preserved differently dependent on where it is observed (C to G).*

## 495 Differential effects of stratigraphy on modes of evolution

496 The extent to which stratigraphic series of trait values are affected by the architecture of the  
497 carbonate platform strongly depends on the mode of evolution (*Figure 6, Supplementary*  
498 *Figures 4–12*). For the same scenario and position in the platform, lineages evolving  
499 according to the stasis model are unaffected by stratigraphy. In contrast, hiatuses introduce  
500 jumps into the lineages evolving according to a weak and strong Brownian drift, which are  
501 not present in the time domain. For the Brownian motion, the presence of jumps depends on  
502 whether the trait series accumulates sufficient trait differences during the hiatus, making the  
503 presence or absence of jumps over gaps effectively random (*Figure 6, B & F, red and green*  
504 *vs. blue lineage*). In general, jumps in traits are more pronounced when (1) evolution is more  
505 directional and (2) gaps are longer.



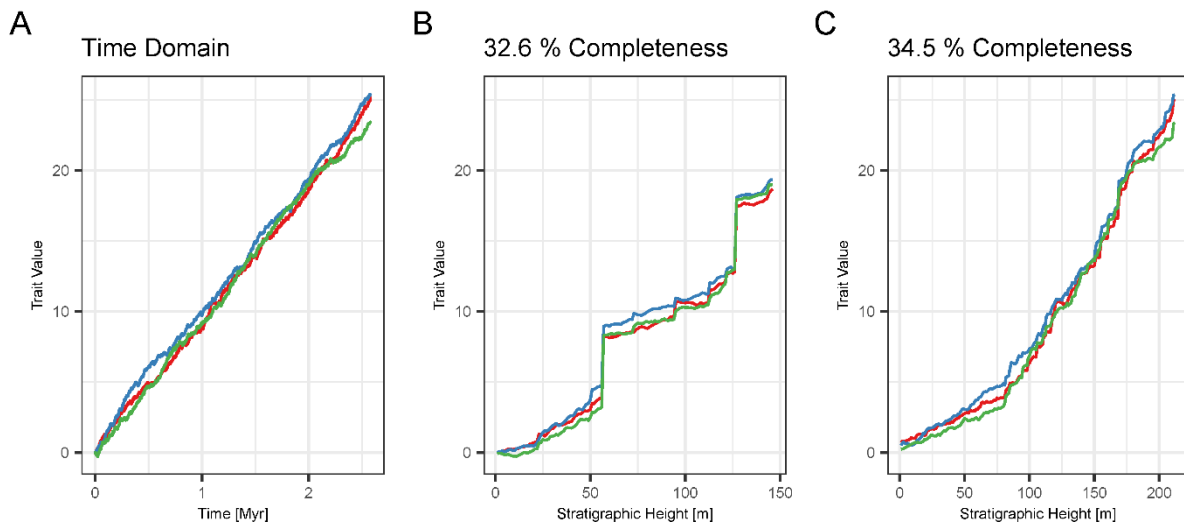
506

507 *Figure 6: Differential preservation of different modes of evolution at the same location. First*  
508 *row: preservation of three lineages evolving according to the stasis (A), Brownian motion*  
509 *(B), weak Brownian drift (C), and strong Brownian drift (D) model 6 km offshore in scenario*  
510 *A. Second row: The corresponding true evolutionary history in the time domain. The change*

511 *in traits observable in fossil time series over a gap depends on the directionality of evolution*  
512 *and gap duration – Stasis is unaffected by the gaps, while the directional weak and strong*  
513 *Brownian drift displays jumps in phenotype over long gaps in the stratigraphic record.*

## 514 **Effects of completeness**

515 Comparing identical modes of evolution at locations in the carbonate platform with similar  
516 stratigraphic completeness shows that stratigraphic completeness is not the major driver of  
517 stratigraphic control ([Figure 7](#)). If hiatuses are frequent and have similar duration, evolution  
518 in the stratigraphic domain is very similar to the time domain. If hiatuses are rare and long,  
519 traits can change significantly during the hiatus, leading to distinct differences in trait values  
520 from before to after the hiatus, generating dissimilarity between observations made in the  
521 stratigraphic domain and the “true” evolutionary history in the time domain.



522

523 *Figure 7 Effects of completeness vs. hiatus duration. Strong Brownian drift in the time*  
524 *domain (A), 2 km offshore in scenario A (B), and 6 km offshore in scenario B (C). In these*  
525 *sections, stratigraphic completeness differs by only 2 %, but preservation of the lineages*

526 *differs drastically due to the presence of few, but long hiatuses in scenario A generated by*  
527 *prolonged intervals of low sea level.*

## 528 **Spatial variation**

529 The stratigraphic expression of trait evolution varies spatially within a carbonate platform  
530 ([Figure 5](#)). This is a direct result of the variability of stratigraphic completeness and hiatus  
531 frequency and duration along the onshore – offshore gradient ([Figure 4](#)). Because of the  
532 selective effects of stratigraphic architectures on the identifiability of directional evolution,  
533 spatial variability is most pronounced for weak and strong Brownian drift, and absent for  
534 stasis (*Supplementary Figures 14–19*).

## 535 **Identification of modes of evolution**

536 Surprisingly, neither the stratigraphic architecture driven by different sea-level histories nor  
537 the location along the onshore-offshore gradient has an influence on the best supported mode  
538 of evolution recovered by the paleoTS package (Hunt 2022). In the absence of stratigraphic  
539 effects, for adequate models, and under excellent sampling conditions (large number of  
540 specimens, low intrapopulation variability in traits, long, equidistant time series), tests fail to  
541 recover the correct (simulated) mode, and support for the correct mode of evolution decreases  
542 as time series length increases.

## 543 **Test results in the stratigraphic domain**

544 In the stratigraphic domain, the tests rarely yielded good support for the correct mode of  
545 evolution as defined by AICc weight > 0.9 (Portet 2020). This holds for both scenarios and  
546 all locations within the carbonate platform ([Figures 8](#) and [9](#), top rows).

547 Under simulated stasis ([Figure 8 A](#) and [Figure 9 A](#)), AICc weight values for the correct  
548 mode of evolution are low (between 0.1 and 0.25). The mode of evolution best supported is  
549 OU with AICc weight values larger than 0.75. This is independent of the location in the  
550 carbonate platform and scenario, except for scenario A, 12 km from shore. Here, AICc  
551 weights are around 0.5 for OU, 0.3 for stasis, and 0.1 for undirected random walk (URW).

552 Under simulated Brownian motion ([Figure 8 B](#) and [Figure 9 B](#)), AICc weights are moderate  
553 to low for all modes of evolution and have high dispersion. For the correct mode of evolution,  
554 URW, AICc weights are around 0.5. For stasis and OU, weights are around 0.25. This is  
555 independent of the location in the platform and of the scenario.

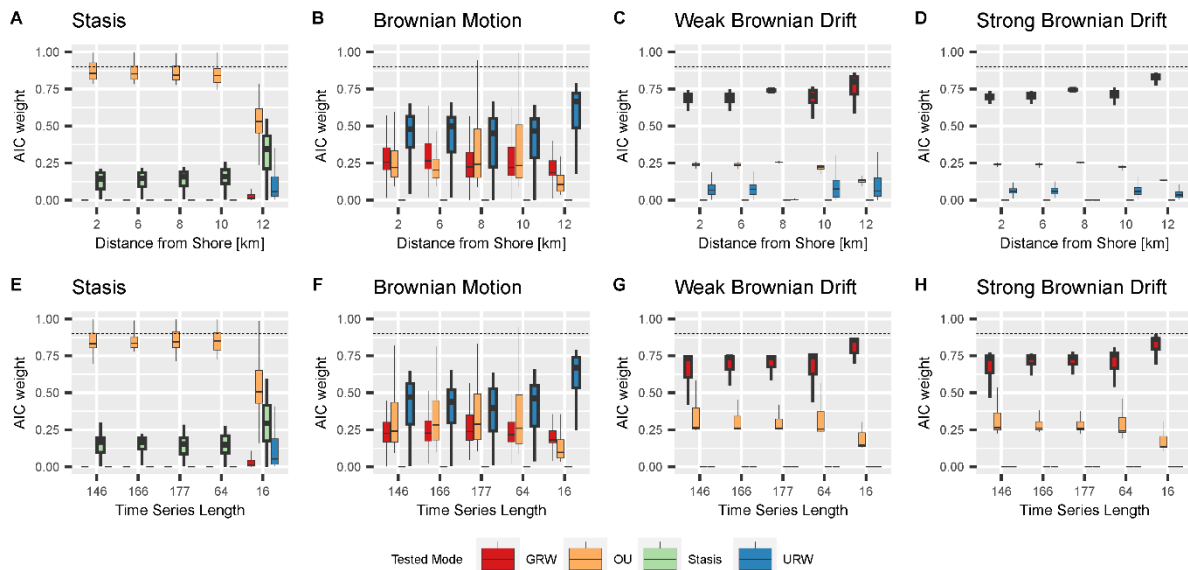
556 Results for simulations of weak and strong Brownian drift are very similar ([Figure 8 C, D](#)  
557 and [Figure 9 C, D](#)). AICc weights for the correct mode of evolution (GRW) are around 0.75,  
558 whereas weights for OU are around 0.25. This holds across both scenarios and all locations in  
559 the platform, with the exception of scenario A, where minor support is found for undirected  
560 random walk (URW).

561 Overall, we find that neither the stratigraphic scenario nor the location in the platform (and,  
562 as consequence, stratigraphic completeness) have a strong effect on the test results.

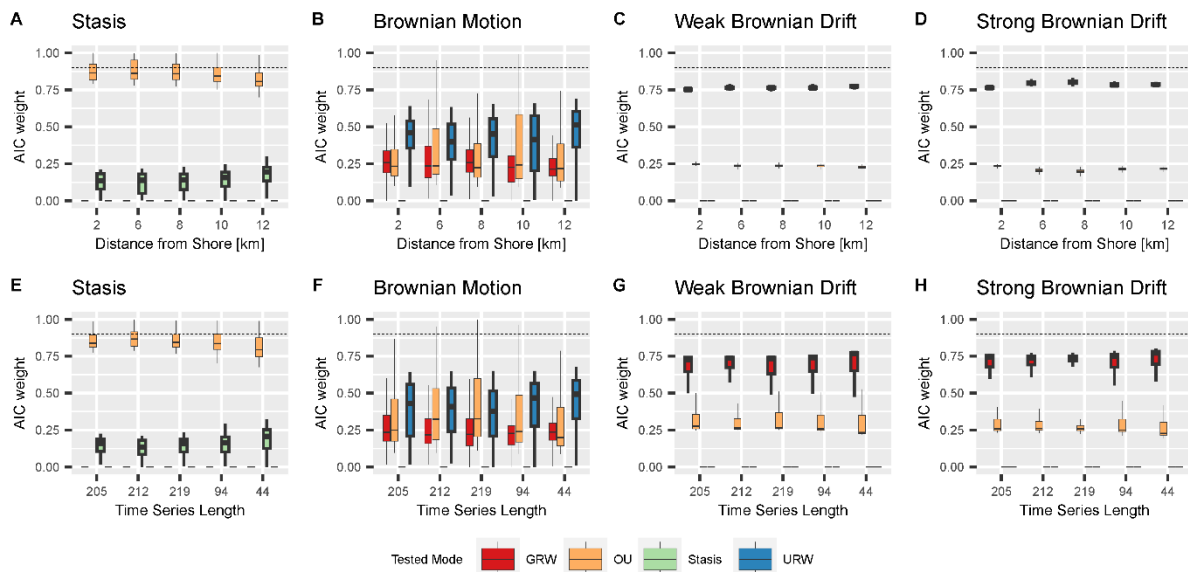
### 563 **Difference between the stratigraphic and time domains**

564 After accounting for time series lengths, we find that test results with and without  
565 stratigraphic effects are very similar ([Figure 8](#) and [Figure 9](#), comparison between the top and  
566 bottom rows). Differences in test results between the time domain and the stratigraphic  
567 domain are (1) weak support for URW under simulations of weak and strong Brownian drift  
568 in scenario A in the stratigraphic domain, while tests in the time domain yield weak support

569 for OU, and (2) lower dispersion of AICc weights in scenario B under simulations of weak  
 570 and strong Brownian drift in the stratigraphic domain compared to the time domain.



572 *Figure 8 AICc weights of different modes of evolution in the stratigraphic domain in scenario*  
 573 *A (first column, A-D) and for time series of equal length, but without stratigraphic biases*  
 574 *(second column, E-H) under simulated stasis (first row), Brownian motion (second row),*  
 575 *weak Brownian drift (third row), and strong Brownian drift (fourth row) at different positions*  
 576 *in the platform. The dashed line indicates the threshold for good support (AICc weight >*  
 577 *0.9), the highlighted boxes are the correct test result for the simulated mode of evolution.*  
 578 *Abbreviations for the tested modes are: GRW - general random walk, OU – Ornstein-*  
 579 *Uhlenbeck process, Stasis – stasis, URW – undirected random walk.*



580

581 *Figure 9: AICc weights of different modes of evolution in the stratigraphic domain in*  
 582 *scenario B (first column, A-D) and for time series of equal length, but without stratigraphic*  
 583 *biases (second column, E-H) under simulated stasis (first row), Brownian motion (second*  
 584 *row), weak Brownian drift (third row), and strong Brownian drift (fourth row) at different*  
 585 *positions in the platform. The dashed line indicates the threshold for good support (AICc*  
 586 *weight > 0.9), the highlighted boxes are the correct test result for the simulated mode of*  
 587 *evolution. Abbreviations for the tested modes are: GRW - general random walk, OU –*  
 588 *Ornstein-Uhlenbeck process, Stasis – stasis, URW – undirected random walk*

## 589 Test performance without stratigraphic biases

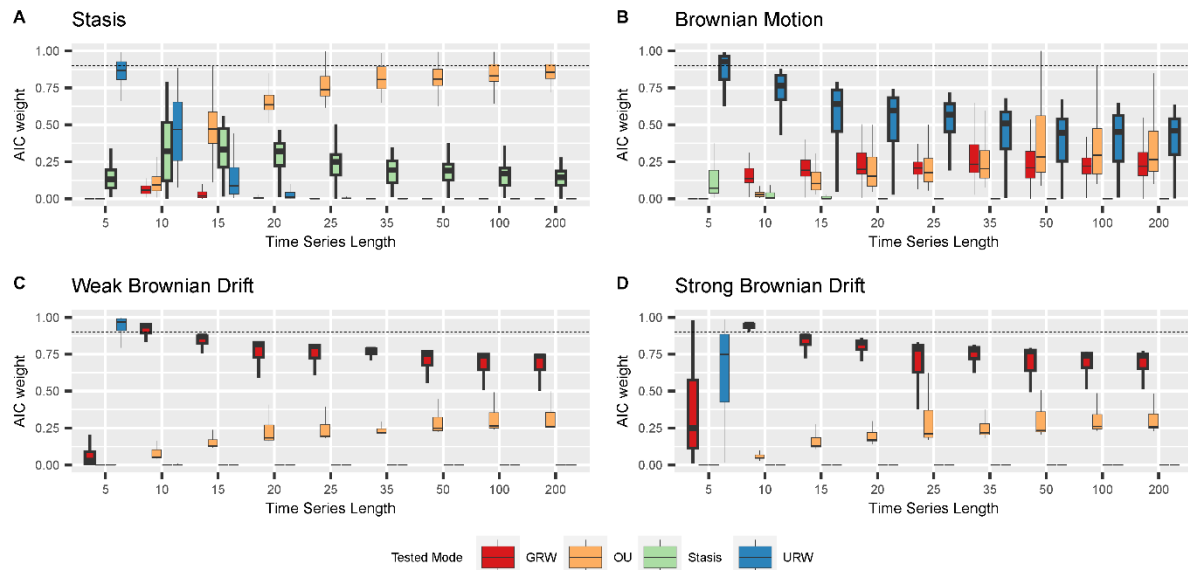
590 Testing for the mode of evolution without stratigraphic effects (i.e., in the time domain), we  
 591 found that increasing sampling resolution (time series length) from 5 to 200 sampling points  
 592 per simulation time reduced support for the correct mode of evolution as measured by AICc  
 593 weights ([Figure 10](#), [Supplementary Figure 20](#)). The results for scenario A ([Figure 10](#)) and  
 594 scenario B ([Supplementary Figure 20](#)) were very similar, thus we focus on scenario A here.

595 Under simulated stasis ([Figure 10 A](#)) AICc weights under low sampling effort (low number  
596 of sampling points) support URW, but this support quickly decreases and eventually vanishes  
597 for more than 20 sampling points. Support for the correct mode of evolution, stasis, peaks at  
598 10 to 15 sampling points at a mean AICc weight of around 0.3, decreases monotonously as  
599 sampling effort is further increased and stabilizes around 0.15. Support for stasis never  
600 reaches the threshold value of 0.9. For time series with 15 or more samples, the AICc weights  
601 are the highest for OU and a portion of them exceeds the 0.9 threshold set as the criterion for  
602 good support. Support for GRW is low to none across all sampling resolutions.

603 Under simulated Brownian motion ([Figure 10 B](#)), support for the correct mode of evolution  
604 (URW) is high for low sampling effort and mostly above 0.9 for series of five samples. It  
605 decreases monotonously to about 0.4 as sampling effort increases. Conversely, support for  
606 both OU and GRW increases monotonously until a mean of 0.25 as sampling effort increases.  
607 Support for stasis is low to null.

608 The results for weak and strong Brownian drift are similar ([Figure 10 C and D](#)). Initial high  
609 (mostly  $>0.9$  in the case of weak Brownian drift) support for URW vanishes with increasing  
610 number of sampling points. In all cases, support for OU increases with sampling effort.  
611 Support for the correct mode of evolution is high under low sampling effort, but decreases as  
612 sampling effort is increased, stabilizing at values around 0.7. Conversely, support for OU  
613 increases monotonously up to a mean of ca. 0.25 as sampling density is increased.





614

615 *Figure 10: AICc weights of modes of evolution in the time domain under simulations of (A)*  
 616 *stasis; (B) Brownian motion; (C) weak Brownian drift; (D) strong Brownian drift as a*  
 617 *function of time series length. The sampled time interval is 2 Ma long (corresponding to the*  
 618 *duration of scenario A), and is sampled with increasing frequency to reflect increasing*  
 619 *sampling efforts. The dashed line indicates the threshold for good support (AICc weight >*  
 620 *0.9), the highlighted boxes are the correct test result for the simulated mode of evolution.*  
 621 *Abbreviations for the tested modes are: GRW - general random walk, OU – Ornstein-*  
 622 *Uhlenbeck process, Stasis – stasis, URW – undirected random walk*

623 In summary, we find that in the absence of stratigraphic effects, the test correctly identified  
 624 the mode of evolution in a portion of simulations when sampling intensity was very low (5  
 625 points) and only for Brownian motion and weak and strong Brownian drift. In the case of  
 626 stasis, the correct mode has never been identified correctly if the threshold of 0.9 AICc  
 627 weight is applied. Support for the correct mode of evolution decreases with time series  
 628 length (Figure 10, Supplementary Figure 20). We thus reject the hypothesis that longer time series  
 629 provide for better identification of the mode of evolution.

## 630 **Discussion**

631 Simulating the preservation of trait evolution in incomplete records formed in carbonate  
632 platforms, we found that – independently of the simulated mode of evolution, the presence or  
633 absence of stratigraphic effects, time series length, or location in the carbonate platform –  
634 tests for the mode of evolution failed to identify the correct mode of evolution according to  
635 the applied criterion of an AICc weight above 0.9 (Portet 2020), and support for the correct  
636 mode of evolution decreases with time series length. Visually, it is not stratigraphic  
637 completeness, but rather maximum hiatus duration and directionality of evolution that  
638 determine how much series of trait values derived from the stratigraphic record differ from  
639 the true evolutionary history.

### 640 **Identifying the mode of evolution from fossil time series**

641 We tested the hypothesis that the mode of evolution identified in a fossil time series obtained  
642 under the assumption of uninterrupted constant sediment accumulation (UCSA) is the same  
643 as the mode of the original time series in the time domain (the “true” evolutionary history).  
644 Although AICc weights of fossil time series derived under this assumption are identical to the  
645 AICc weights of the true evolutionary history, the tests fail to identify the correct mode of  
646 evolution based on the initially set criterion of an AICc weight larger than 0.9 for both  
647 stratigraphies studied here ([Figure 8](#) and [Figure 9](#)). Spatial variability in AICc weights in  
648 both carbonate platforms can be explained by differences in time series length resulting from  
649 differences in total accumulated thickness ([Figure 10](#)) rather than differences in stratigraphic  
650 architectures. Because of the inability of the test to identify the correct mode of evolution in  
651 the absence of any stratigraphic effects, our first hypothesis proved untestable with the

652 chosen approach. This test behavior is not due to our implementations of models of  
653 phenotypic evolution, as it persists when the internal simulation procedures provided by the  
654 paleoTS package are used (Hohmann and Hopkins 2024). This suggests that the test  
655 commonly yields an incorrect mode beyond our own study.

656 One possible explanation for the poor performance of the tests is that they are based on the  
657 Akaike information criterion (AICc), which measures relative fit of models to data. In the  
658 stratigraphic domain, none of the standard models of phenotypic evolution adequately  
659 describe the data. For example, the stratigraphic expression of the Brownian drift models  
660 resembles a Lévy process with rare, but large, jumps, rather than a Brownian drift (Landis,  
661 Schraiber, and Liang 2013; Landis and Schraiber 2017) ([Figure 5](#)). The issues arising from  
662 using AICc when models are not adequate are well known, and the adequacy of models of  
663 phyletic evolution has been discussed by Voje, Starrfelt and Liow (2018) and (Voje 2018),  
664 While they do not provide a general definition of what it means for a model to be adequate,  
665 they propose four tests for adequacy of models of phyletic evolution. In the time domain, we  
666 simulate lineages according to the same model we test for. Accordingly, the models must be  
667 adequate to describe the data as they generated the data in the first place, yet the test do not  
668 find good support for the correct mode of evolution. Another possible explanation for our  
669 inability to recover the correct simulated mode of evolution is that our definition of what it  
670 means to identify a model is too strict. Other criteria for good fit of a model are available (see  
671 e.g. Hopkins and Lidgard (2012)). However, this does not explain why, in the absence of  
672 stratigraphic biases, support for the correct mode as measured by AICc weights decrease as  
673 time series get longer (Figures [8](#) and [9](#), lower row, [Figure 10](#)) — a qualitative behavior that is  
674 independent of any threshold for good model support.. For time series longer than 15  
675 observations, support for the correct mode of evolution measured by AICc weights decreases  
676 ([Figure 10](#), [Supplementary Figure 20](#)). Based on the probabilistic interpretation of the AICc

677 weights, this implies that the more samples are collected, the lower the probability that the  
678 data-generating model is the best model (Wagenmakers and Farrell 2004). One explanation  
679 for this apparent statistical paradox is that sampling a fixed time interval more frequently  
680 leads to diminishing returns on the information gain per sample. Intuitively, a few samples  
681 should be sufficient to separate directional evolution from stasis. However, this does not  
682 explain why AICc weights for the correct mode of evolution decrease instead of increase.  
683 Another potential explanation is that AIC is not consistent in the sense that if sample size  
684 grows, the probability that AIC identifies the true model does not approach one (Bozdogan  
685 1987). It is unclear if the considered time series are long enough to display such asymptotic  
686 effects, and how they translate from AIC to AICc weights.

687 There is an ongoing debate about the usage of Ornstein-Uhlenbeck models in phylogenetic  
688 comparative approaches (Ho and Ané 2014). Cooper et al. (2016) argue that OU processes  
689 are frequently incorrectly favored over simpler processes, while Grabowski et al. (2023)  
690 argue that this position is unsubstantiated. Using model selection, we found increasing  
691 support for OU as time series length increases. One potential explanation for this might be  
692 that OU processes contain many other processes as non-nested endmembers: With no  
693 selection, they are an unbiased random walk (Cooper et al. 2016), with a distant phenotypic  
694 optimum they resemble directional evolution with noise, and when starting at the phenotypic  
695 optimum they represent (autocorrelated) stasis.

696 Summarizing, we cannot resolve why tests do not identify the correct mode of evolution,  
697 longer time series yield lower AICc weights for the correct mode of evolution, and AICc  
698 weights are unaffected by stratigraphic biases.

## 699 **Effects of stratigraphic incompleteness**

700 The second hypothesis we examined was that the lower the stratigraphic completeness, the  
701 lower the chance to identify the correct mode of evolution from fossil time series that are  
702 constructed based on the assumption of uninterrupted constant sediment accumulation  
703 (UCSA). Because of the inability of the tests to find support for the correct mode of evolution  
704 in the absence of stratigraphic biases, we visually compared fossil time series derived under  
705 this assumption with time series of the true evolutionary history (*Figures 5, 6, 7,*  
706 *Supplementary Figures 4–19*).

707 Trait evolution reconstructed using simplified age-depth models varies spatially throughout  
708 the platform (*Figure 5*). Even if gaps are identified and their duration is known, evolutionary  
709 history coinciding with sea level drops is not preserved on the platform top. These time  
710 intervals can be recovered from the distal slope where sediment is continuously accreted  
711 during lowstand shedding (*Figures 3 and 4*) (Grammer and Ginsburg 1992). This highlights  
712 the importance to combine information from across the entire sedimentary basin to  
713 reconstruct past changes (Holland and Patzkowsky 2015; Zimmt et al. 2021), although the  
714 information gained from this approach might vary between carbonate platforms and  
715 siliciclastic systems.

716 We found that stratigraphic incompleteness (Dingus and Sadler 1982; Tipper 1987) is an  
717 imperfect measure to quantify the biasing effects of stratigraphic architectures on phenotypic  
718 evolution. For similar values of stratigraphic completeness, the stratigraphic expression of the  
719 same lineage can strongly differ. For example, fossil time series of Brownian drift reflect the  
720 underlying true evolutionary history, or display apparent jumps in phenotype for very close  
721 values of completeness (*Figure 7*). In addition, different modes of evolution are biased to a  
722 different degree when compared within the same section (and thus identical stratigraphic

723 effects and values of incompleteness). For example, in the same section Brownian drift  
724 displays jumps in phenotype over gaps that will be misinterpreted as elevated rates of  
725 evolution, whereas stasis remains unaffected ([Figure 6](#)). Multiple definitions of  
726 incompleteness have been applied in stratigraphy (Anders, Krueger, and Sadler 1987), some  
727 of which incorporate spatial variability (Straub and Foreman 2018). The definition of  
728 stratigraphic completeness from (Tipper 1987) we used here reflects the intuition that gaps in  
729 the geological record are the dominant factor that diminishes the quality of the fossil record.  
730 While other definitions of incompleteness might be more suitable to quantifying stratigraphic  
731 effects, our results show that the nature of the underlying evolutionary process cannot be  
732 neglected when assessing the fidelity of the fossil record.

733 The change of phenotype over a gap is determined by gap duration and the change in  
734 phenotype accumulated over this time interval. Stasis remains unaffected by gaps as it  
735 accumulates no change in phenotype. On the other hand, for Brownian drift models, change  
736 in phenotype is proportional to gap duration. Under the simplified assumptions on ADMs we  
737 used, the change in traits over gaps will be taken at face value, giving trait evolution a distinct  
738 punctuated look (Rita et al. 2019). While a precise modern formulation of the punctuated  
739 equilibrium hypothesis (Gould and Eldredge 1972) is debated (see Pennell, Harmon, and  
740 Uyeda (2014) vs. Lieberman and Eldredge (2014)), these jumps will be mistaken for intervals  
741 with elevated evolutionary rates. Models of trait evolution that can incorporate punctuations  
742 are Lévy processes, a class of stochastic process that combines gradual change with discrete  
743 jumps (Landis, Schraiber, and Liang 2013; Landis and Schraiber 2017). In Lévy processes,  
744 the jump components are random and have a Poisson structure. This provides a way to  
745 separate between artefactual jumps introduced by simplistic ADMs and true elevated rates of  
746 evolution: Artefactual jumps will coincide with gaps in the record or interval of reduced  
747 sediment accumulation rates, and thus connect to external drivers of stratigraphic

748 architectures such as drops in sea level, rather than being random. Our study provides the  
749 stratigraphic null hypothesis that punctuated equilibrium should be more prevalent at times  
750 with low frequency sea-level changes. Combined, our results suggest that due to gaps in the  
751 stratigraphic record, fossil time series favor the recognition of both stasis and complex,  
752 punctuated models of evolution (Hunt, Hopkins, and Lidgard 2015).  
753 Hoffman (1989) pointed out that most paleontological evidence for punctuated equilibrium  
754 comes from shallow water habitats (e.g. (Kelley 1983; Williamson 1981)), which they argue  
755 are more incomplete and thus favor the recognition of punctuations. This reflects the common  
756 idea that different environments have different incompleteness and thus different abilities to  
757 preserve evolution, as we have phrased in our hypothesis two. In contrast to this  
758 preconception, we found that many environments in a carbonate platform have very similar  
759 incompleteness and hiatus distributions ([Figure 4](#)). Due to the flat geometry of the platform,  
760 the separation is between platform top and slope, not the distinct environments within the  
761 platform such as forereef and lagoonal environments (Liu and Liu 2021). In addition,  
762 incompleteness alone is not sufficient to produce artefactual jumps in phenotype ([Figure 7](#)).  
763 Gaps in the stratigraphic record need to be sufficiently long compared to the rate of the  
764 evolutionary process, so that morphologies can change enough to display sufficient offset  
765 over the gap. This indicates that, rather than incompleteness, maximum hiatus duration is  
766 driving the discrepancy between fossil time series and the true evolutionary history.  
767 Naturally, maximum hiatus duration is limited by stratigraphic completeness and the time  
768 covered by the section. But even under high incompleteness, as long as hiatus frequency is  
769 high and durations are short, the fossil record can still give a good insight into evolutionary  
770 history, and be adequate to test a wide range of evolutionary hypotheses (Paul 1992).  
771 In our stratigraphic models, hiatus frequency and duration are determined by the frequency of  
772 sea-level fluctuations. Preservation of evolutionary history under high-frequency sea level

773 changes (scenario B) is good, while the large-scale fluctuations in scenario A result in  
774 prolonged gaps with a large impact on the recovery of the mode of evolution (Figure 7). This  
775 demonstrates that understanding controls on the spatial and temporal heterogeneity of the  
776 stratigraphic record is decisive in correctly interpreting the evolutionary history of a lineage  
777 in the realistic case of spatially constrained sampling.

## 778 **Limitations of the simulated carbonate platforms**

779 Carbonate platforms used for this research only approximate stratigraphic architectures that  
780 would form in nature. First, CarboCAT Lite does not include erosion other than sediment  
781 transport, which removes sediment locally immediately after its formation, but preserves the  
782 total volume of generated sediment in the platform. In real carbonate platforms, part of the  
783 carbonate sediment is dissolved and returned to the water column (e.g., Albright, Langdon,  
784 and Anthony (2013), exported into the ocean, and a part is chemically and mechanically  
785 eroded when it becomes emerged. The addition of erosion to the model would have the effect  
786 of enlarging the present gaps in the record and merging the shorter ones, resulting in fewer,  
787 longer gaps and lower stratigraphic completeness. Second, carbonate production curves used  
788 to inform the models reflect activities of carbonate factories under stable conditions. In  
789 reality, a regression would often lead to removal of carbonate producing organisms from the  
790 emerged area. The recolonization of this area by carbonate producers would lead to a lag in  
791 the factory resuming its activity. Carbonate production and preservation is also sensitive to  
792 diurnal, seasonal and long-term astronomical cycles, e.g. through temperature control over  
793 the proportion of precipitated aragonite (Balthasar and Cusack 2015) and the length of the  
794 vegetative season of calcifiers (e.g., Marshall and Clode 2004; Mancuso et al. 2019).  
795 Our simulations did not include pelagic carbonate production, spatially heterogeneous  
796 subsidence or gravitational sediment transport, which may be crucial in the formation of



797 some empirical carbonate platforms (Masiero et al. 2020). We relied here on high benthic *in*  
798 *situ* production rates as the dominant driver of sediment accumulation in tropical, attached  
799 carbonate platforms. Thus, the stratigraphic architectures presented here are conceptual  
800 endpoints with exaggerated completeness.

801 The construction of our study follows the assumption of uninterrupted constant sediment  
802 accumulation (UCSA), which implies that the ages of fossils found at a given stratigraphic  
803 position correspond to the age of the stratum. This assumption is made in many simulation  
804 studies of trait evolution in the fossil record (e.g. (Hannisdal 2006)) and inherent to most  
805 methods that estimate age-depth models (e.g. (Parnell et al. 2008)). With this respect, our  
806 computer experiment is representative for such studies. However, time averaging and  
807 sedimentary condensation mean that typically more time is represented by fossils than by  
808 sedimentary strata (Kowalewski and Bambach 2008; Tomašových et al. 2022). On the other  
809 hand, fossils of different ages will be found at the same stratigraphic height, limiting the  
810 temporal resolution of evolutionary steps in the population's mean. Because of high *in situ*  
811 sediment production, timescales of time averaging identified in modern tropical carbonate  
812 environments are typically much shorter than rates of trait evolution, regardless of the way  
813 they are measured (Hunt 2012; Voje 2016; Kowalewski et al. 2017; Philip D. Gingerich  
814 2019). This means that trait evolution reconstructed in tropical carbonate platforms may not  
815 be representative for other environments with lower rates of sediment accumulation or higher  
816 proportion of transported material.

## 817 **Conclusions**

818 We tested the hypothesis that the commonly employed approach to identifying the mode of  
819 evolution in fossil succession, i.e. linear projection of stratigraphic positions of occurrences

820 into the time domain without considering changes in sedimentation rate and gaps in the  
821 record, recovers the correct mode of evolution. In the course of the study, it appeared that the  
822 test is, in fact, not possible, because the commonly used test does not recover the correct  
823 mode of evolution even from complete data (i.e. if the time domain is sampled without gaps  
824 or distortions). In both considered situations: original mode of evolution in time and its  
825 distorted record in the stratigraphic domain, the tests did not yield clear support for the  
826 correct mode of evolution. Our findings differ from those of Hannisdal (2006) , who found  
827 (using a different approach but asking the same question) that incomplete sampling in the  
828 stratigraphic record may result in all other modes of evolution being identified as stasis. In  
829 our study, we never found strong support for stasis.

830 Our findings did not vary substantially between two stratigraphic architectures with varying  
831 gap distributions and degrees of stratigraphic completeness. The difficulty in identifying the  
832 correct mode of evolution holds across depositional environments. This is counterintuitive, as  
833 deeper environments are often assumed to be more complete and therefore more suitable for  
834 sampling fossil series for evolutionary studies. Increasing the number of observations (i.e.  
835 sampling intensity, length of the fossil series) did not improve the identification of the mode  
836 of evolution, but rather worsened it.

837 Our study was motivated by improving the recovery of evolutionary information from highly-  
838 resolve fossil successions, particularly at microevolutionary scales. We are convinced that  
839 such successions can aliment models and understanding that is not accessible to exclusively  
840 neontological methodologies, as illustrated by e.g. Hopkins and Lidgard (2012); Voje (2016);  
841 Petryshen et al. (2020). Our contribution is the use of stratigraphic forward modeling to  
842 ground-truth the methodologies serving this palaeobiological research program. Forward  
843 modeling allows rigorous testing of concerns that the fossil record is too distorted, or too  
844 incomplete, to answer (micro)evolutionary questions. The conclusion of our study is,

845 unexpectedly, that it may be the analytical methods that limit our use of fossil data, rather  
846 than the quality of the fossil record. The proliferation of ever better stratigraphic forward  
847 models (e.g. CarboCAT (P. M. Burgess 2013; Masiero et al. 2020), SedFlux (Hutton and  
848 Syvitski 2008), strataR (Holland 2022), CarboKitten.jl (Hidding et al., 2024)) opens the  
849 possibility to validate these methods and improve our understanding of the fossil record.

## 850 **Acknowledgements**

851 The authors would like to thank Melanie Hopkins, Katharine Loughney, Bjarte Hannisdal,  
852 Kenneth De Baets, and one anonymous reviewer for their feedback on the manuscript. The  
853 authors would also like to thank the Peer Community In (PCI) Paleontology.

## 854 **Declarations**

### 855 **Ethics approval and consent to participate**

856 Not applicable

### 857 **Consent for publication**

858 Not applicable

### 859 **Availability of data and materials**

860 The dataset supporting the conclusions of this article is available in the Zenodo repository,  
861 <https://doi.org/10.17605/OSF.IO/ZBPWA> (Hohmann, Koelewijn, and Jarochovska 2023a).

862 All code used can be found in Hohmann, Koelewijn, and Jarochovska (2023b) and is

863 accessible via <https://doi.org/10.5281/zenodo.10390267>. Supplementary figures can be found  
864 in the supplementary materials.

## 865 **Competing interests**

866 The authors declare that they have no competing interests

## 867 **Funding**

868 Funded by the European Union (ERC, MindTheGap, StG project no 101041077). Views and  
869 opinions expressed are however those of the author(s) only and do not necessarily reflect  
870 those of the European Union or the European Research Council. Neither the European Union  
871 nor the granting authority can be held responsible for them.

## 872 **Authors' contributions**

873 According to the CRediT taxonomy

874 **Niklas Hohmann:** Conceptualization, Methodology, Software, Validation, Formal analysis,  
875 Investigation, Data curation, Writing – Original Draft, Writing – Review & Editing,  
876 Visualization.

877 **Joël R. Koelewijn:** Software, Validation, Formal analysis, Investigation, Visualization.

878 **Peter Burgess:** Writing – Review & Editing, Software.

879 **Emilia Jarochovska:** Conceptualization, Methodology, Validation, Visualization, Writing –  
880 Review & Editing, Supervision, Project administration, Funding acquisition.

## 881 **References**

- 882 Albright, R., C. Langdon, and K. R. N. Anthony. 2013. “Dynamics of Seawater Carbonate  
883 Chemistry, Production, and Calcification of a Coral Reef Flat, Central Great Barrier  
884 Reef.” *Biogeosciences* 10 (10): 6747–58. <https://doi.org/10.5194/bg-10-6747-2013>.  
885 Anders, Mark H., Scot W. Krueger, and Peter M. Sadler. 1987. “A New Look at  
886 Sedimentation Rates and the Completeness of the Stratigraphic Record.” *The Journal*  
887 *of Geology* 95 (1): 1–14. <https://doi.org/10.1086/629103>.  
888 Aze, Tracy, Thomas H. G. Ezard, Andy Purvis, Helen K. Coxall, Duncan R. M. Stewart,  
889 Bridget S. Wade, and Paul N. Pearson. 2011. “A Phylogeny of Cenozoic  
890 Macroperforate Planktonic Foraminifera from Fossil Data.” *Biological Reviews* 86  
891 (4): 900–927. <https://doi.org/10.1111/j.1469-185X.2011.00178.x>.

- 892 Balthasar, Uwe, and Maggie Cusack. 2015. "Aragonite-Calcite Seas—Quantifying the Gray  
893 Area." *Geology* 43 (2): 99–102. <https://doi.org/10.1130/G36293.1>.
- 894 Barido-Sottani, Joëlle, Alexander Pohle, Kenneth De Baets, Duncan Murdock, and Rachel C.  
895 M. Warnock. 2023. "Putting the F into FBD Analysis: Tree Constraints or  
896 Morphological Data?" *Palaeontology* 66 (6): e12679.  
897 <https://doi.org/10.1111/pala.12679>.
- 898 Barido-Sottani, Joëlle, Nina M. A. van Tiel, Melanie J. Hopkins, David F. Wright, Tanja  
899 Stadler, and Rachel C. M. Warnock. 2020. "Ignoring Fossil Age Uncertainty Leads to  
900 Inaccurate Topology and Divergence Time Estimates in Time Calibrated Tree  
901 Inference." *Frontiers in Ecology and Evolution* 8.  
902 <https://www.frontiersin.org/articles/10.3389/fevo.2020.00183>.
- 903 Beran, Jan. 2017. *Mathematical Foundations of Time Series Analysis: A Concise*  
904 *Introduction*. Cham: Springer International Publishing. <https://doi.org/10.1007/978-3-319-74380-6>.
- 905
- 906 Bookstein, Fred L. 1987. "Random Walk and the Existence of Evolutionary Rates."  
907 *Paleobiology* 13 (4): 446–64. <https://doi.org/10.1017/S0094837300009039>.
- 908 Bosscher, Hemmo, and Wolfgang Schlager. 1992. "Computer Simulation of Reef Growth."  
909 *Sedimentology* 39 (3): 503–12. <https://doi.org/10.1111/j.1365-3091.1992.tb02130.x>.
- 910 Bozdogan, Hamparsum. 1987. "Model Selection and Akaike's Information Criterion (AIC):  
911 The General Theory and Its Analytical Extensions." *Psychometrika* 52 (3): 345–70.  
912 <https://doi.org/10.1007/BF02294361>.
- 913 Burgess, Peter. (2023) 2023. "CarboCAT Lite." MATLAB. [https://github.com/MindTheGap-](https://github.com/MindTheGap-ERC/CarboCATLite)  
914 [ERC/CarboCATLite](https://github.com/MindTheGap-ERC/CarboCATLite).
- 915 Burgess, Peter M. 2013. "CarboCAT: A Cellular Automata Model of Heterogeneous  
916 Carbonate Strata." *Computers & Geosciences, Modeling for Environmental Change*,  
917 53 (April): 129–40. <https://doi.org/10.1016/j.cageo.2011.08.026>.
- 918 Clyde, William C., and Philip D. Gingerich. 1994. "Rates of Evolution in the Dentition of  
919 Early Eocene Cantius: Comparison of Size and Shape." *Paleobiology* 20 (4): 506–22.  
920 <https://doi.org/10.1017/S0094837300012963>.
- 921 Cooper, Natalie, Gavin H. Thomas, Chris Venditti, Andrew Meade, and Rob P. Freckleton.  
922 2016. "A Cautionary Note on the Use of Ornstein Uhlenbeck Models in  
923 Macroevolutionary Studies." *Biological Journal of the Linnean Society* 118 (1): 64–  
924 77. <https://doi.org/10.1111/bij.12701>.
- 925 Darwin, Charles. 1859. *On the Origin of Species: A Facsimile of the First Edition*. Harvard  
926 University Press.
- 927 Dingus, Lowell, and Peter M. Sadler. 1982. "The Effects of Stratigraphic Completeness on  
928 Estimates of Evolutionary Rates." *Systematic Biology* 31 (4): 400–412.  
929 <https://doi.org/10.1093/sysbio/31.4.400>.
- 930 Donoghue, Philip C. J. 2001. "Conodonts Meet Cladistics: Recovering Relationships and  
931 Assessing the Completeness of the Conodont Fossil Record." *Palaeontology* 44 (1):  
932 65–93. <https://doi.org/10.1111/1475-4983.00170>.
- 933 Dzik, Jerzy. 1985. "Typologic versus Population Concepts of Chronospecies : Implications  
934 for Ammonite Biostratigraphy." *Acta Palaeontologica Polonica* 30 (1–2): 71–92.
- 935 ———. 1995. "Range-Based Biostratigraphy and Evolutionary Geochronology."  
936 *Paleopelagos Special Publication* 1 (94): 121–28.
- 937 ———. 1999. "Relationship between Rates of Speciation and Phyletic Evolution:  
938 Stratophenetic Data on Pelagic Conodont Chordates and Benthic Ostracods." *Geobios*  
939 32 (2): 205–21. [https://doi.org/10.1016/S0016-6995\(99\)80033-3](https://doi.org/10.1016/S0016-6995(99)80033-3).
- 940 ———. 2005. "The Chronophyletic Approach: Stratophenetics Facing an Incomplete Fossil  
941 Record." *Special Papers in Palaeontology* 73: 159–83.

- 942 Gingerich, P.D. 1983. "Rates of Evolution: Effects of Time and Temporal Scaling." *Science*  
943 222: 159–62.
- 944 ———. 2001. "Rates of Evolution on the Time Scale of the Evolutionary Process." In  
945 *Microevolution Rate, Pattern, Process*, edited by A. P. Hendry and M. T. Kinnison,  
946 127–44. Contemporary Issues in Genetics and Evolution. Dordrecht: Springer  
947 Netherlands. [https://doi.org/10.1007/978-94-010-0585-2\\_9](https://doi.org/10.1007/978-94-010-0585-2_9).
- 948 Gingerich, Philip D. 2019. *Rates of Evolution: A Quantitative Synthesis*. Cambridge:  
949 Cambridge University Press. <https://doi.org/10.1017/9781316711644>.
- 950 Gingerich, Philip D., and Margaret Schoeninger. 1977. "The Fossil Record and Primate  
951 Phylogeny." *Journal of Human Evolution* 6 (5): 483–505.  
952 [https://doi.org/10.1016/S0047-2484\(77\)80059-6](https://doi.org/10.1016/S0047-2484(77)80059-6).
- 953 Gould, Stephen Jay, and Niles Eldredge. 1972. "Punctuated Equilibria: An Alternative to  
954 Phyletic Gradualism." *Models in Paleobiology* 1972: 82–115.
- 955 Grabowski, Mark, Jason Pienaar, Kjetil L Voje, Staffan Andersson, Jesualdo Fuentes-  
956 González, Bjørn T Kopperud, Daniel S Moen, Masahito Tsuboi, Josef Uyeda, and  
957 Thomas F Hansen. 2023. "A Cautionary Note on 'A Cautionary Note on the Use of  
958 Ornstein Uhlenbeck Models in Macroevolutionary Studies.'" *Systematic Biology* 72  
959 (4): 955–63. <https://doi.org/10.1093/sysbio/syad012>.
- 960 Grammer, G. Michael, and Robert N. Ginsburg. 1992. "Highstand versus Lowstand  
961 Deposition on Carbonate Platform Margins: Insight from Quaternary Foreslopes in  
962 the Bahamas." *Marine Geology* 103 (1): 125–36. [https://doi.org/10.1016/0025-3227\(92\)90012-7](https://doi.org/10.1016/0025-3227(92)90012-7).
- 964 Grantham, Todd. 2004. "The Role of Fossils in Phylogeny Reconstruction: Why Is It so  
965 Difficult to Integrate Paleobiological and Neontological Evolutionary Biology?"  
966 *Biology and Philosophy* 19 (5): 687–720. <https://doi.org/10.1007/s10539-005-0370-z>.
- 967 Guenser, Pauline, Rachel C. M. Warnock, Walker Pett, Philip C. J. Donoghue, and Emilia  
968 Jarochovska. 2021. "Does Time Matter in Phylogeny? A Perspective from the Fossil  
969 Record." bioRxiv. <https://doi.org/10.1101/2021.06.11.445746>.
- 970 Hannisdal, Bjarte. 2006. "Phenotypic Evolution in the Fossil Record: Numerical  
971 Experiments." *The Journal of Geology* 114 (2): 133–53.  
972 <https://doi.org/10.1086/499569>.
- 973 Haug, Joachim Tobias, and Carolin Haug. 2017. "Species, Populations and Morphotypes  
974 through Time – Challenges and Possible Concepts." Edited by Sylvain Charbonnier.  
975 *BSGF - Earth Sciences Bulletin* 188 (3): 20. <https://doi.org/10.1051/bsgf/2017181>.
- 976 Hidding, Johan, Emilia Jarochovska, Xianyi Liu, Peter Burgess, Niklas Hohmann, and  
977 Hanno Spreeuw. 2024. "CarboKitten.JL."
- 978 Ho, Lam Si Tung, and Cécile Ané. 2014. "Intrinsic Inference Difficulties for Trait Evolution  
979 with Ornstein-Uhlenbeck Models." *Methods in Ecology and Evolution* 5 (11): 1133–  
980 46. <https://doi.org/10.1111/2041-210X.12285>.
- 981 Hoffman, Antoni. 1989. *Arguments on Evolution: A Paleontologist's Perspective*. New York:  
982 Oxford University Press.
- 983 Hohmann, Niklas. 2021. "Incorporating Information on Varying Sedimentation Rates into  
984 Paleontological Analyses." *PALAIOS* 36 (2): 53–67.  
985 <https://doi.org/10.2110/palo.2020.038>.
- 986 Hohmann, Niklas, and Melanie Hopkins. 2024. "paleoTS\_test: Examine paleoTS Model  
987 Selection Performance with Time Series Length." [object Object].  
988 <https://doi.org/10.5281/ZENODO.10843692>.
- 989 Hohmann, Niklas, Jan R. Koelewijn, and Emilia Jarochovska. 2023a. "Identification of the  
990 Mode of Evolution in Incomplete Carbonate Successions - Supporting Data." Open  
991 Science Framework. <https://doi.org/10.17605/OSF.IO/ZBPWA>.

- 992 ———. 2023b. “Identification of the Mode of Evolution in Incomplete Carbonate  
993 Successions - Supporting Code.” Zernodo. <https://doi.org/10.5281/zenodo.10390266>.
- 994 Holland, Steven M. 2022. “The Structure of the Nonmarine Fossil Record: Predictions from a  
995 Coupled Stratigraphic–Paleoecological Model of a Coastal Basin.” *Paleobiology* 48  
996 (3): 372–96. <https://doi.org/10.1017/pab.2022.5>.
- 997 Holland, Steven M., and Mark E. Patzkowsky. 2015. “The Stratigraphy of Mass Extinction.”  
998 *Palaeontology* 58 (5): 903–24. <https://doi.org/10.1111/pala.12188>.
- 999 Hopkins, Melanie J., and Scott Lidgard. 2012. “Evolutionary Mode Routinely Varies among  
1000 Morphological Traits within Fossil Species Lineages.” *Proceedings of the National  
1001 Academy of Sciences* 109 (50): 20520–25. <https://doi.org/10.1073/pnas.1209901109>.
- 1002 Hunt, Gene. 2006. “Fitting and Comparing Models of Phyletic Evolution: Random Walks  
1003 and Beyond.” *Paleobiology* 32 (4): 578–601. <https://doi.org/10.1666/05070.1>.
- 1004 ———. 2010. “Evolution in Fossil Lineages: Paleontology and The Origin of Species.” *The  
1005 American Naturalist* 176 (S1): S61–76. <https://doi.org/10.1086/657057>.
- 1006 ———. 2012. “Measuring Rates of Phenotypic Evolution and the Inseparability of Tempo  
1007 and Mode.” *Paleobiology* 38 (3): 351–73.
- 1008 ———. 2022. “paleoTS: Analyze Paleontological Time-Series.” [https://CRAN.R-  
1009 project.org/package=paleoTS](https://CRAN.R-project.org/package=paleoTS).
- 1010 Hunt, Gene, Melanie J. Hopkins, and Scott Lidgard. 2015. “Simple versus Complex Models  
1011 of Trait Evolution and Stasis as a Response to Environmental Change.” *Proceedings  
1012 of the National Academy of Sciences of the United States of America* 112 (16): 4885–  
1013 90. <https://doi.org/10.1073/pnas.1403662111>.
- 1014 Hunt, Gene, and Kaustuv Roy. 2006. “Climate Change, Body Size Evolution, and Cope’s  
1015 Rule in Deep-Sea Ostracodes.” *Proceedings of the National Academy of Sciences* 103  
1016 (5): 1347–52. <https://doi.org/10.1073/pnas.0510550103>.
- 1017 Hutton, Eric W. H., and James P. M. Syvitski. 2008. “Sedflux 2.0: An Advanced Process-  
1018 Response Model That Generates Three-Dimensional Stratigraphy.” *Computers &  
1019 Geosciences, Predictive Modeling in Sediment Transport and Stratigraphy*, 34 (10):  
1020 1319–37. <https://doi.org/10.1016/j.cageo.2008.02.013>.
- 1021 Jablonski, David, Kaustuv Roy, and James W. Valentine. 2006. “Out of the Tropics:  
1022 Evolutionary Dynamics of the Latitudinal Diversity Gradient.” *Science* 314 (5796):  
1023 102–6. <https://doi.org/10.1126/science.1130880>.
- 1024 Jones, David. 2009. “Directional Evolution in the Conodont *Pterospirifer*.” *Paleobiology*  
1025 35 (3): 413–31.
- 1026 Kelley, Patricia H. 1983. “Evolutionary Patterns of Eight Chesapeake Group Molluscs:  
1027 Evidence for the Model of Punctuated Equilibria.” *Journal of Paleontology* 57 (3):  
1028 581–98.
- 1029 Kemp, David B. 2012. “Stochastic and Deterministic Controls on Stratigraphic Completeness  
1030 and Fidelity.” *International Journal of Earth Sciences* 101 (8): 2225–38.  
1031 <https://doi.org/10.1007/s00531-012-0784-1>.
- 1032 Kidwell, Susan M., and Karl W. Flessa. 1996. “The Quality of the Fossil Record:  
1033 Populations, Species, and Communities.” *Annual Review of Earth and Planetary  
1034 Sciences* 24 (1): 433–64. <https://doi.org/10.1146/annurev.earth.24.1.433>.
- 1035 Kidwell, Susan M., and Steven M. Holland. 2002. “The Quality of the Fossil Record:  
1036 Implications for Evolutionary Analyses.” *Annual Review of Ecology and Systematics*  
1037 33 (1): 561–88. <https://doi.org/10.1146/annurev.ecolsys.33.030602.152151>.
- 1038 Kowalewski, Michał, and Richard K. Bambach. 2008. “The Limits of Paleontological  
1039 Resolution.” In *High-Resolution Approaches in Stratigraphic Paleontology*, edited by  
1040 P. J. Harries, 21:1–48. Topics in Geobiology. Dordrecht: Springer Netherlands.  
1041 [https://doi.org/10.1007/978-1-4020-9053-0\\_1](https://doi.org/10.1007/978-1-4020-9053-0_1).

- 1042 Kowalewski, Michał, Sahale Casebolt, Quan Hua, Katherine E. Whitacre, Darrell S.  
1043 Kaufman, and Matthew A. Kosnik. 2017. “One Fossil Record, Multiple Time  
1044 Resolutions: Disparate Time-Averaging of Echinoids and Mollusks on a Holocene  
1045 Carbonate Platform.” *Geology* 46 (1): 51–54. <https://doi.org/10.1130/G39789.1>.
- 1046 Lande, Russell. 1976. “Natural Selection and Random Genetic Drift in Phenotypic  
1047 Evolution.” *Evolution* 30 (2): 314–34. <https://doi.org/10.2307/2407703>.
- 1048 Landis, Michael J., and Joshua G. Schraiber. 2017. “Pulsed Evolution Shaped Modern  
1049 Vertebrate Body Sizes.” *Proceedings of the National Academy of Sciences* 114 (50):  
1050 13224–29. <https://doi.org/10.1073/pnas.1710920114>.
- 1051 Landis, Michael J., Joshua G. Schraiber, and Mason Liang. 2013. “Phylogenetic Analysis  
1052 Using Lévy Processes: Finding Jumps in the Evolution of Continuous Traits.”  
1053 *Systematic Biology* 62 (2): 193–204. <https://doi.org/10.1093/sysbio/sys086>.
- 1054 Lieberman, Bruce S., and Niles Eldredge. 2014. “What Is Punctuated Equilibrium? What Is  
1055 Macroevolution? A Response to Pennell et Al.” *Trends in Ecology & Evolution* 29  
1056 (4): 185–86. <https://doi.org/10.1016/j.tree.2014.02.005>.
- 1057 Liu, Jianliang, and Keyu Liu. 2021. “Estimating Stratal Completeness of Carbonate  
1058 Deposition via Process-Based Stratigraphic Forward Modeling.” *Science China Earth  
1059 Sciences* 64 (2): 253–59. <https://doi.org/10.1007/s11430-020-9660-8>.
- 1060 MacLeod, Norman. 1991. “Punctuated Anagenesis and the Importance of Stratigraphy to  
1061 Paleobiology.” *Paleobiology* 17 (2): 167–88.  
1062 <https://doi.org/10.1017/S0094837300010472>.
- 1063 Malmgren, Björn A., W. A. Berggren, and G. P. Lohmann. 1983. “Evidence for Punctuated  
1064 Gradualism in the Late Neogene Globorotalia Tumida Lineage of Planktonic  
1065 Foraminifera.” *Paleobiology* 9 (4): 377–89.  
1066 <https://doi.org/10.1017/S0094837300007843>.
- 1067 Mancuso, Arianna, Marco Stagoni, Fiorella Prada, Daniele Scarponi, Corrado Piccinetti, and  
1068 Stefano Goffredo. 2019. “Environmental Influence on Calcification of the Bivalve  
1069 Chamelea Gallina along a Latitudinal Gradient in the Adriatic Sea.” *Scientific Reports*  
1070 9 (1): 11198. <https://doi.org/10.1038/s41598-019-47538-1>.
- 1071 Marshall, A.T., and P. Clode. 2004. “Calcification Rate and the Effect of Temperature in a  
1072 Zooxanthellate and an Azooxanthellate Scleractinian Reef Coral.” *Coral Reefs* 23 (2):  
1073 218–24. <https://doi.org/10.1007/s00338-004-0369-y>.
- 1074 Masiero, Isabella, Estanislao Kozłowski, Georgios Antonatos, Haiwei Xi, and Peter Burgess.  
1075 2020. “Numerical Stratigraphic Forward Models as Conceptual Knowledge  
1076 Repositories and Experimental Tools: An Example Using a New Enhanced Version of  
1077 CarboCAT.” *Computers & Geosciences* 138 (May): 104453.  
1078 <https://doi.org/10.1016/j.cageo.2020.104453>.
- 1079 McNeill, Donald F. 2005. “Accumulation Rates from Well-Dated Late Neogene Carbonate  
1080 Platforms and Margins.” *Sedimentary Geology, Sedimentology in the 21st Century -  
1081 A Tribute to Wolfgang Schlager*, 175 (1): 73–87.  
1082 <https://doi.org/10.1016/j.sedgeo.2004.12.032>.
- 1083 Miller, Kenneth G., James V. Browning, W. John Schmelz, Robert E. Kopp, Gregory S.  
1084 Mountain, and James D. Wright. 2020. “Cenozoic Sea-Level and Cryospheric  
1085 Evolution from Deep-Sea Geochemical and Continental Margin Records.” *Science  
1086 Advances* 6 (20): eaaz1346. <https://doi.org/10.1126/sciadv.aaz1346>.
- 1087 Mitchell, Jonathan S, Rampal S Etienne, and Daniel L Rabosky. 2019. “Inferring  
1088 Diversification Rate Variation from Phylogenies with Fossils.” *Systematic Biology* 68  
1089 (1): 1–18. <https://doi.org/10.1093/sysbio/syy035>.
- 1090 Mongiardino Koch, Nicolás, Russell J. Garwood, and Luke A. Parry. 2021. “Fossils Improve  
1091 Phylogenetic Analyses of Morphological Characters.” *Proceedings of the Royal*



- 1092 *Society B: Biological Sciences* 288 (1950): 20210044.  
1093 <https://doi.org/10.1098/rspb.2021.0044>.
- 1094 Parnell, A. C., J. Haslett, J. R. M. Allen, C. E. Buck, and B. Huntley. 2008. “A Flexible  
1095 Approach to Assessing Synchronicity of Past Events Using Bayesian Reconstructions  
1096 of Sedimentation History.” *Quaternary Science Reviews* 27 (19): 1872–85.  
1097 <https://doi.org/10.1016/j.quascirev.2008.07.009>.
- 1098 Patterson, Colin. 1981. “Significance of Fossils in Determining Evolutionary Relationships.”  
1099 *Annual Review of Ecology and Systematics* 12: 195–223.
- 1100 Paul, Christopher R. C. 1992. “How Complete Does the Fossil Record Have to Be?” *Revista*  
1101 *Española de Paleontología* 7 (2): 127–33.
- 1102 Pearson, Paul N. 1992. “Survivorship Analysis of Fossil Taxa When Real-Time Extinction  
1103 Rates Vary: The Paleogene Planktonic Foraminifera.” *Paleobiology* 18 (2): 115–31.  
1104 <https://doi.org/10.1017/S0094837300013920>.
- 1105 Pennell, Matthew W., Luke J. Harmon, and Josef C. Uyeda. 2014. “Is There Room for  
1106 Punctuated Equilibrium in Macroevolution?” *Trends in Ecology & Evolution* 29 (1):  
1107 23–32. <https://doi.org/10.1016/j.tree.2013.07.004>.
- 1108 Petryshen, W., C. M. Henderson, K. De Baets, and E. Jarochovska. 2020. “Evidence of  
1109 Parallel Evolution in the Dental Elements of Sweetognathus Conodonts.” *Proceedings*  
1110 *of the Royal Society B: Biological Sciences* 287 (1939): 20201922.  
1111 <https://doi.org/10.1098/rspb.2020.1922>.
- 1112 Platen, Eckhard, and Nicola Bruti-Liberati. 2010. *Numerical Solution of Stochastic*  
1113 *Differential Equations with Jumps in Finance*. Vol. 64. Stochastic Modelling and  
1114 Applied Probability. Berlin, Heidelberg: Springer Berlin Heidelberg.  
1115 <https://doi.org/10.1007/978-3-642-13694-8>.
- 1116 Plint, A. Guy, and Dag Nummedal. 2000. “The Falling Stage Systems Tract: Recognition and  
1117 Importance in Sequence Stratigraphic Analysis.” *Geological Society, London, Special*  
1118 *Publications* 172 (1): 1–17. <https://doi.org/10.1144/GSL.SP.2000.172.01.01>.
- 1119 Portet, Stéphanie. 2020. “A Primer on Model Selection Using the Akaike Information  
1120 Criterion.” *Infectious Disease Modelling* 5: 111–28.  
1121 <https://doi.org/10.1016/j.idm.2019.12.010>.
- 1122 Quental, Tiago B., and Charles R. Marshall. 2010. “Diversity Dynamics: Molecular  
1123 Phylogenies Need the Fossil Record.” *Trends in Ecology & Evolution* 25 (8): 434–41.  
1124 <https://doi.org/10.1016/j.tree.2010.05.002>.
- 1125 R Core Team. 2023. *R: A Language and Environment for Statistical Computing*. Vienna,  
1126 Austria: R Foundation for Statistical Computing. <https://www.R-project.org/>.
- 1127 Rita, Patrícia, Paulina Nätscher, Luís V. Duarte, Robert Weis, and Kenneth De Baets. 2019.  
1128 “Mechanisms and Drivers of Belemnite Body-Size Dynamics across the  
1129 Pliensbachian–Toarcian Crisis.” *Royal Society Open Science* 6 (12): 190494.  
1130 <https://doi.org/10.1098/rsos.190494>.
- 1131 Sheets, H. David, and Charles E. Mitchell. 2001. “Uncorrelated Change Produces the  
1132 Apparent Dependence of Evolutionary Rate on Interval.” *Paleobiology* 27 (3): 429–  
1133 45. [https://doi.org/10.1666/0094-8373\(2001\)027<0429:UCPTAD>2.0.CO;2](https://doi.org/10.1666/0094-8373(2001)027<0429:UCPTAD>2.0.CO;2).
- 1134 Springer, Mark S. 1995. “Molecular Clocks and the Incompleteness of the Fossil Record.”  
1135 *Journal of Molecular Evolution* 41 (5): 531–38. <https://doi.org/10.1007/BF00175810>.
- 1136 Stadler, Tanja, Alexandra Gavryushkina, Rachel C. M. Warnock, Alexei J. Drummond, and  
1137 Tracy A. Heath. 2018. “The Fossilized Birth-Death Model for the Analysis of  
1138 Stratigraphic Range Data under Different Speciation Modes.” *Journal of Theoretical*  
1139 *Biology* 447 (June): 41–55. <https://doi.org/10.1016/j.jtbi.2018.03.005>.

- 1140 Straub, Kyle M., and Brady Z. Foreman. 2018. “Geomorphic Stasis and Spatiotemporal  
1141 Scales of Stratigraphic Completeness.” *Geology* 46 (4): 311–14.  
1142 <https://doi.org/10.1130/G40045.1>.
- 1143 Strömberg, Caroline A. E. 2006. “Evolution of Hypsodonty in Equids: Testing a Hypothesis  
1144 of Adaptation.” *Paleobiology* 32 (2): 236–58. [https://doi.org/10.1666/0094-  
1145 8373\(2006\)32\[236:EOHIET\]2.0.CO;2](https://doi.org/10.1666/0094-8373(2006)32[236:EOHIET]2.0.CO;2).
- 1146 Symonds, Matthew R. E., and Adnan Moussalli. 2011. “A Brief Guide to Model Selection,  
1147 Multimodel Inference and Model Averaging in Behavioural Ecology Using Akaike’s  
1148 Information Criterion.” *Behavioral Ecology and Sociobiology* 65 (1): 13–21.  
1149 <https://doi.org/10.1007/s00265-010-1037-6>.
- 1150 Tipper, John C. 1987. “Estimating Stratigraphic Completeness.” *The Journal of Geology* 95  
1151 (5): 710–15.
- 1152 Tomašových, Adam, Ivo Gallmetzer, Alexandra Haselmair, and Martin Zuschin. 2022.  
1153 “Inferring Time Averaging and Hiatus Durations in the Stratigraphic Record of High-  
1154 frequency Depositional Sequences.” Edited by Christian Betzler. *Sedimentology* 69  
1155 (3): 1083–1118. <https://doi.org/10.1111/sed.12936>.
- 1156 Voje, Kjetil Lysne. 2016. “Tempo Does Not Correlate with Mode in the Fossil Record.”  
1157 *Evolution* 70 (12): 2678–89. <https://doi.org/10.1111/evo.13090>.
- 1158 ———. 2018. “Assessing Adequacy of Models of Phyletic Evolution in the Fossil Record.”  
1159 *Methods in Ecology and Evolution* 9 (12): 2402–13. [https://doi.org/10.1111/2041-  
1160 210X.13083](https://doi.org/10.1111/2041-210X.13083).
- 1161 ———. 2020. “Testing Eco-Evolutionary Predictions Using Fossil Data: Phyletic Evolution  
1162 Following Ecological Opportunity\*.” *Evolution* 74 (1): 188–200.  
1163 <https://doi.org/10.1111/evo.13838>.
- 1164 Voje, Kjetil Lysne, Jostein Starrfelt, and Lee Hsiang Liow. 2018. “Model Adequacy and  
1165 Microevolutionary Explanations for Stasis in the Fossil Record.” *The American  
1166 Naturalist* 191 (4): 509–23. <https://doi.org/10.1086/696265>.
- 1167 Wagenmakers, Eric-Jan, and Simon Farrell. 2004. “AIC Model Selection Using Akaike  
1168 Weights.” *Psychonomic Bulletin & Review* 11 (1): 192–96.  
1169 <https://doi.org/10.3758/BF03206482>.
- 1170 Warnock, Rachel C. M., Tracy A. Heath, and Tanja Stadler. 2020. “Assessing the Impact of  
1171 Incomplete Species Sampling on Estimates of Speciation and Extinction Rates.”  
1172 *Paleobiology* 46 (2): 137–57. <https://doi.org/10.1017/pab.2020.12>.
- 1173 Warrlich, G. M. D. 2000. “3D Computer Forward Modelling of Carbonate Platform  
1174 Evolution.” PhD, London: Royal Holloway University of London.
- 1175 Wehmiller, John F., Daniel F. Belknap, Brian S. Boutin, June E. Mirecki, Stephen D.  
1176 Rahaim, and Linda L. York. 1988. “A Review of the Aminostratigraphy of  
1177 Quaternary Mollusks from United States Atlantic Coastal Plain Sites.” In *Dating  
1178 Quaternary Sediments*, edited by Don J. Easterbrook, 227:0. Geological Society of  
1179 America. <https://doi.org/10.1130/SPE227-p69>.
- 1180 Wilkinson, Bruce H., Bradley N. Opdyke, and Thomas J. Algeo. 1991. “Time Partitioning in  
1181 Cratonic Carbonate Rocks.” *Geology* 19 (11): 1093–96. [https://doi.org/10.1130/0091-  
1182 7613\(1991\)019<1093:TPICCR>2.3.CO;2](https://doi.org/10.1130/0091-7613(1991)019<1093:TPICCR>2.3.CO;2).
- 1183 Williamson, P. G. 1981. “Palaeontological Documentation of Speciation in Cenozoic  
1184 Molluscs from Turkana Basin.” *Nature* 293 (5832): 437–43.  
1185 <https://doi.org/10.1038/293437a0>.
- 1186 Wills, Matthew A. 1999. “Congruence Between Phylogeny and Stratigraphy: Randomization  
1187 Tests and the Gap Excess Ratio.” Edited by C. Marshall. *Systematic Biology* 48 (3):  
1188 559–80. <https://doi.org/10.1080/106351599260148>.

- 1189 Wright, April M., David W. Bapst, Joëlle Barido-Sottani, and Rachel C.M. Warnock. 2022.  
1190 “Integrating Fossil Observations Into Phylogenetics Using the Fossilized Birth–Death  
1191 Model.” *Annual Review of Ecology, Evolution, and Systematics* 53 (1): 251–73.  
1192 <https://doi.org/10.1146/annurev-ecolsys-102220-030855>.  
1193 Zimmt, Joshua B., Steven M. Holland, Seth Finnegan, and Charles R. Marshall. 2021.  
1194 “Recognizing Pulses of Extinction from Clusters of Last Occurrences.” *Palaeontology*  
1195 64 (1): 1–20. <https://doi.org/10.1111/pala.12505>.  
1196